Magnétisme et sa première application

Chapitres 2 et 4

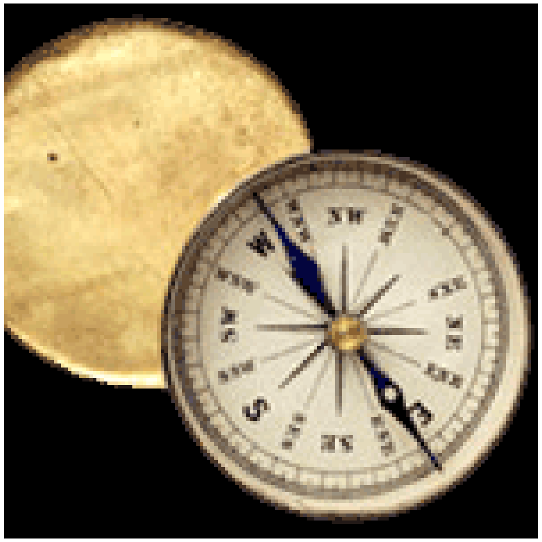

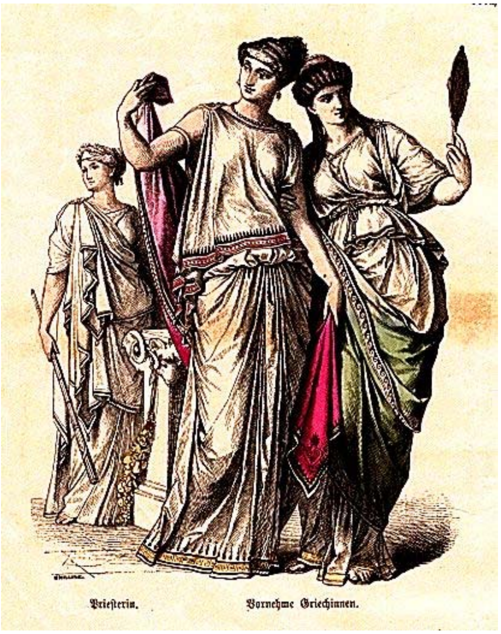

12ème siècle, compréhension ~ 1600

Le fer magnétique était connu
des savants grecs 1000 ans AD

Applications

Isolant magnétique en théorie des solides standard?

Physique du solide standard: métal, isolant

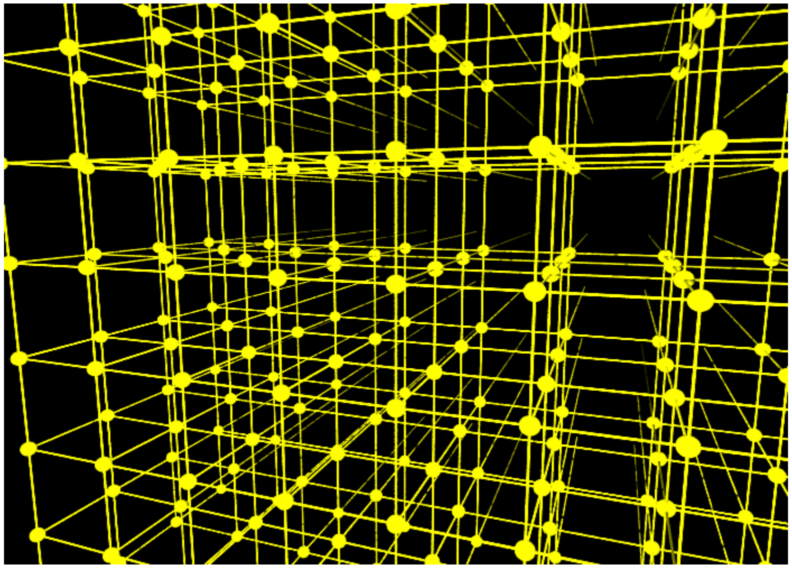

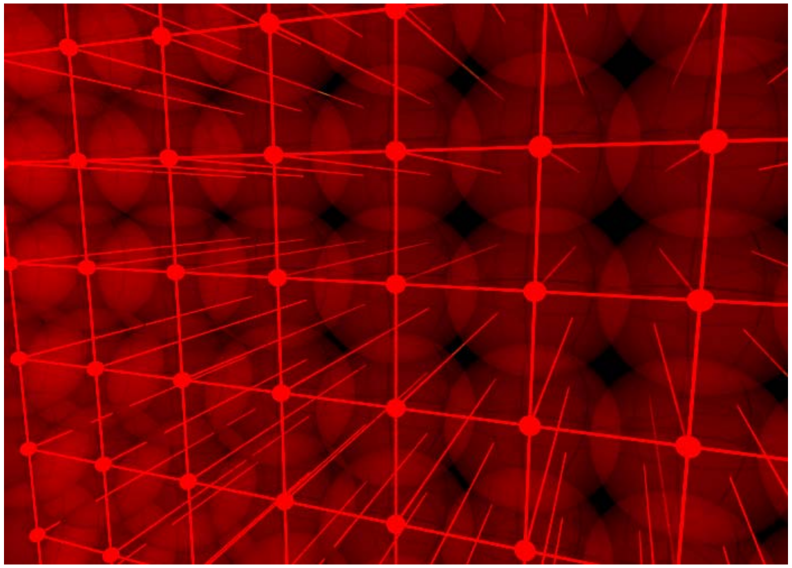

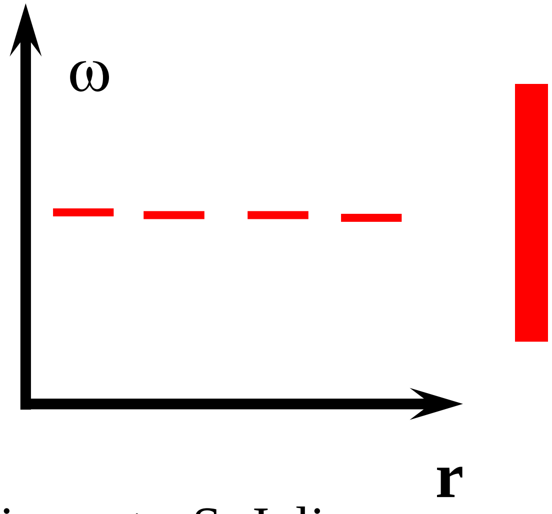

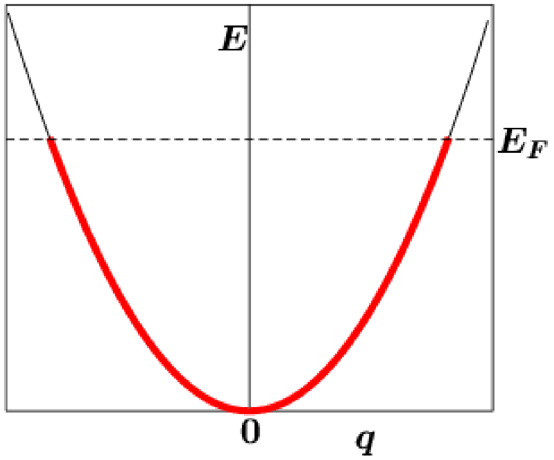

Remerciements, S. Julian

Remplir la mer de Fermi

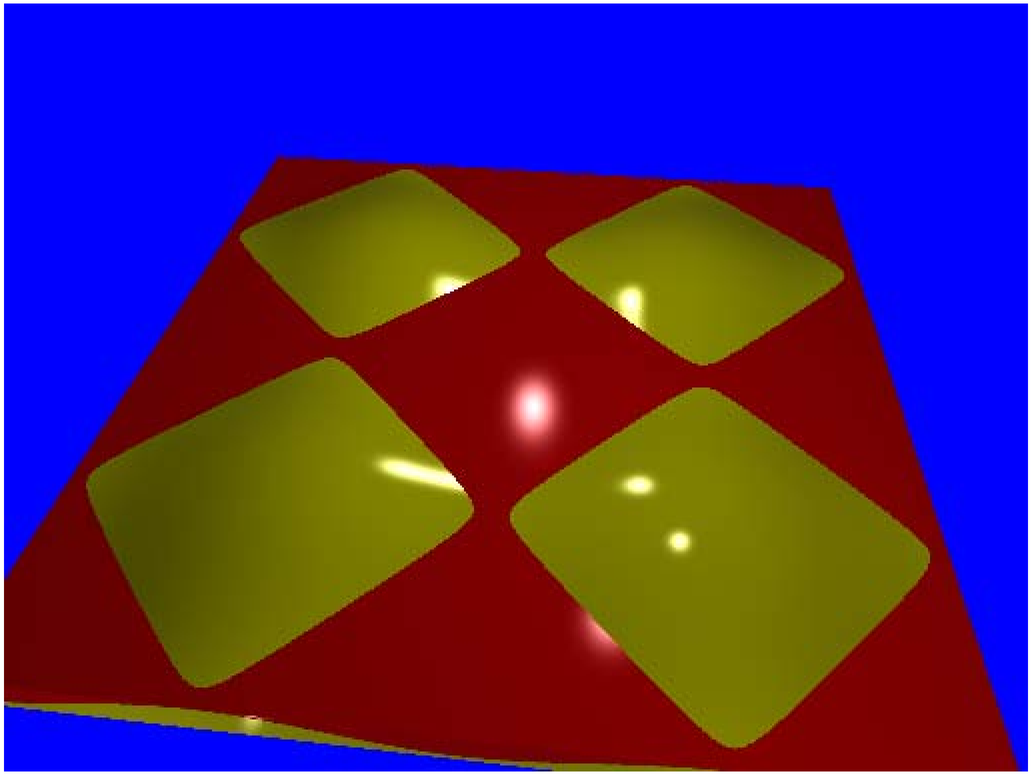

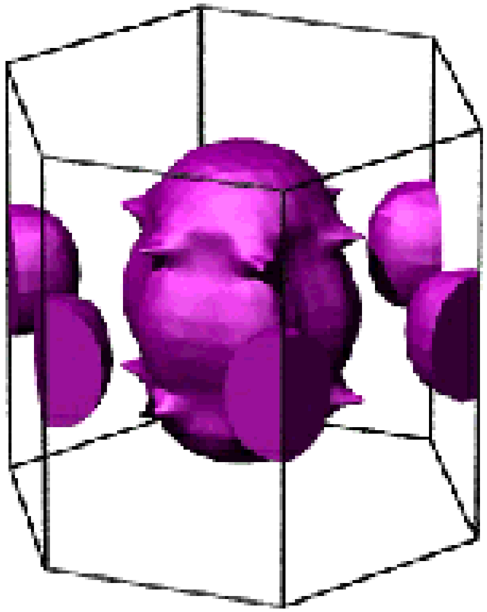

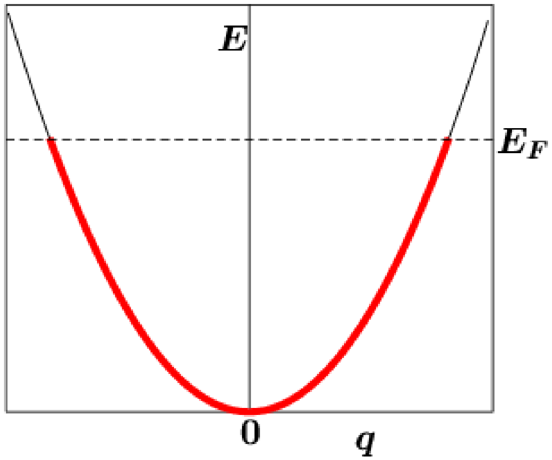

Remerciements, S. Julian

Une découverte, 1911

- Heike Kamerlingh Onnes (1853/1926)

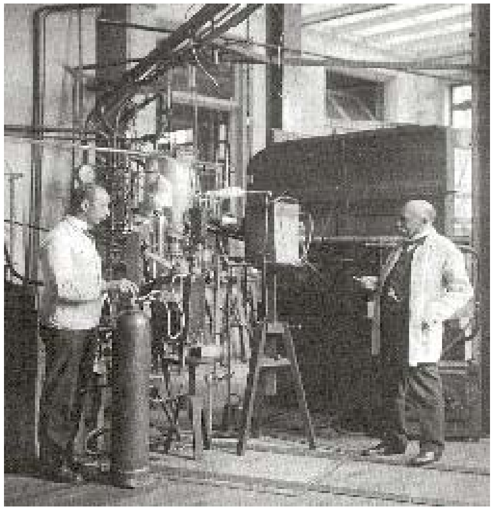

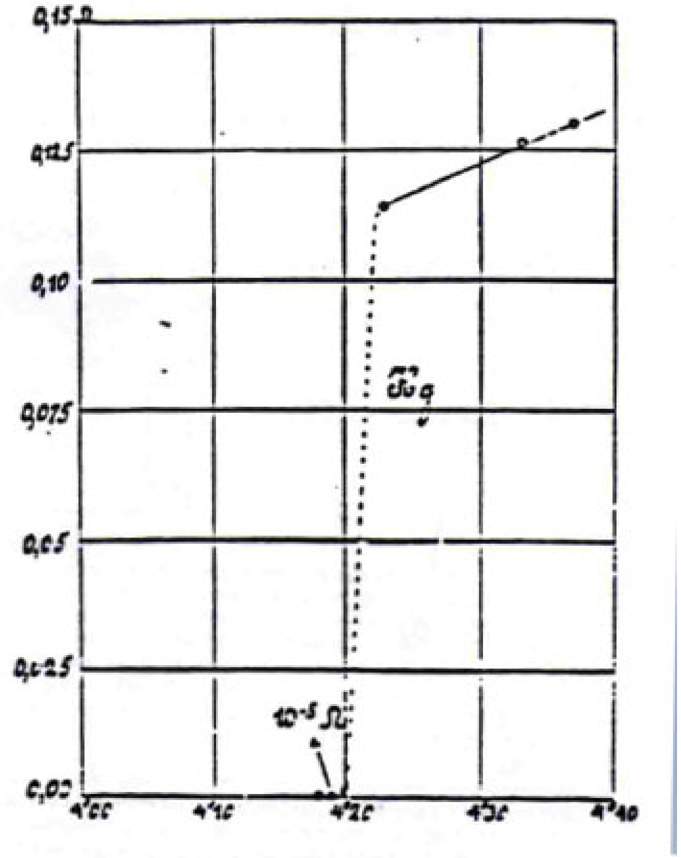

Un métal parfait?

Supraconductivité : La découverte, 1911

- Heike Kamerlingh Onnes (1853/1926)
  - Cryogénie
  - Premier à liquéfier l'He (4 K)
  - Nobel de physique (1913)
- Étudie la résistance des matériaux purs à *T=0*
  - Supraconductivité de *Hg* en 1911, puis *Sn* et *Pb*

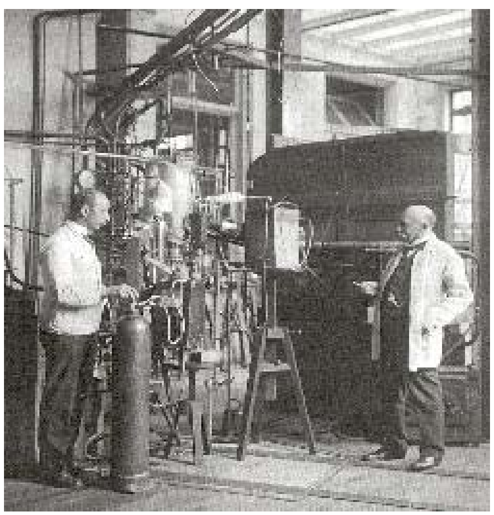

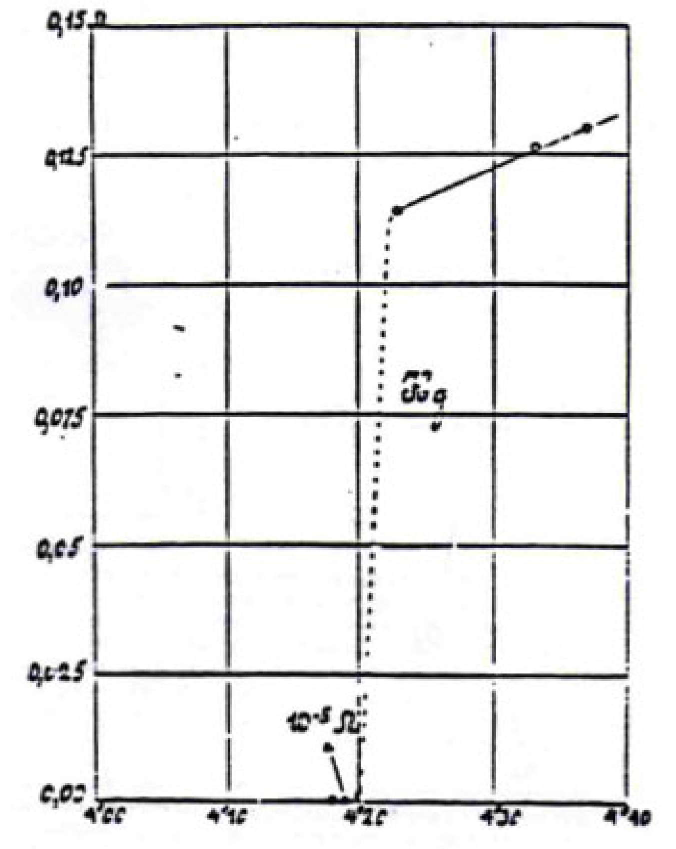

Métal parfait et supraconducteur?

- Expérience numéro 1
  - Appliquer un champ magnétique à haute température
  - Refroidir sous Tc
- Expérience numéro 2
  - Refroidir sous Tc
  - Appliquer un champ magnétique
- Deux expériences, deux résultats pour un conducteur parfait
- Même résultat pour un supraconducteur !

Détection de champs magnétiques faibles

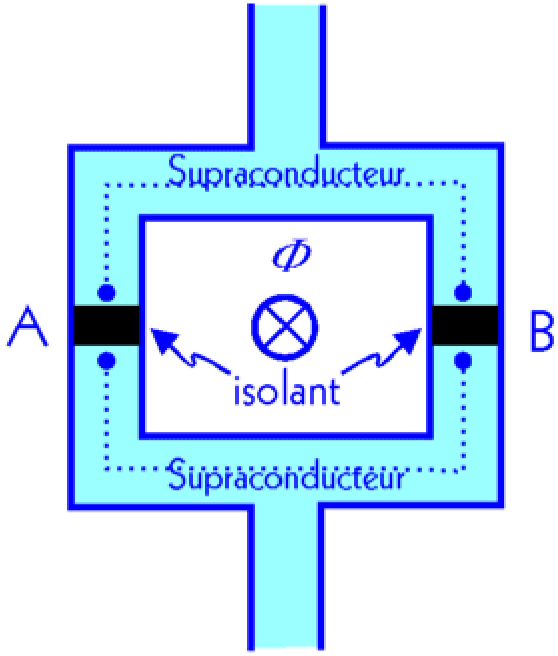

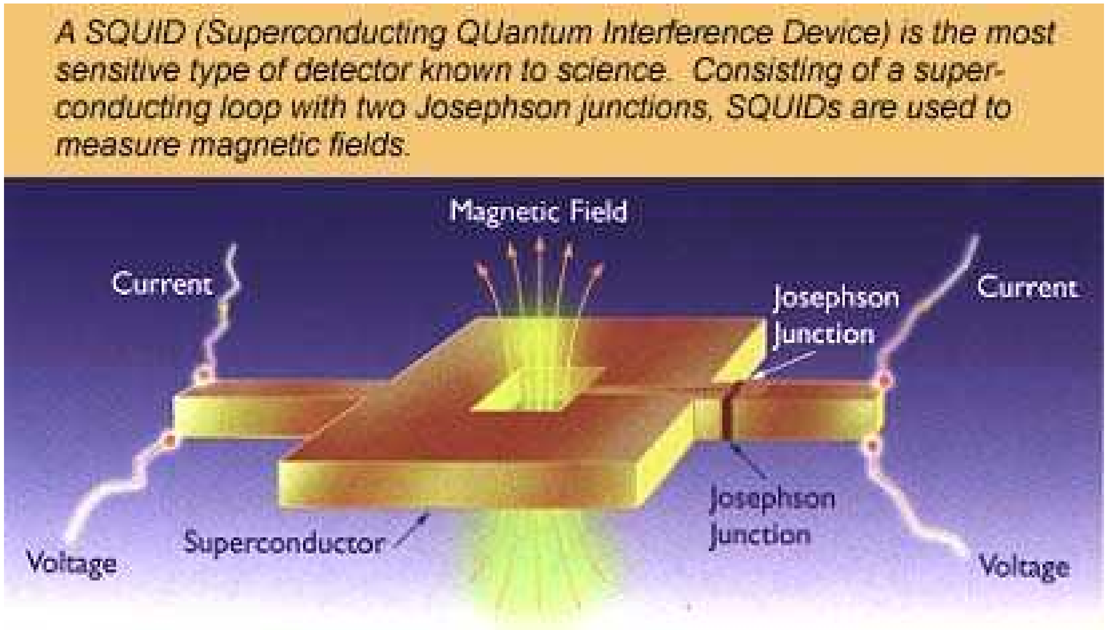

SQUID "Superconducting Quantum Interference Device"

Un champ magnétique modifie la phase des ondes de matière. En détectant les oscillations dans le courant, on peut détecter des champs magnétiques très faibles.

Lignes à transmission

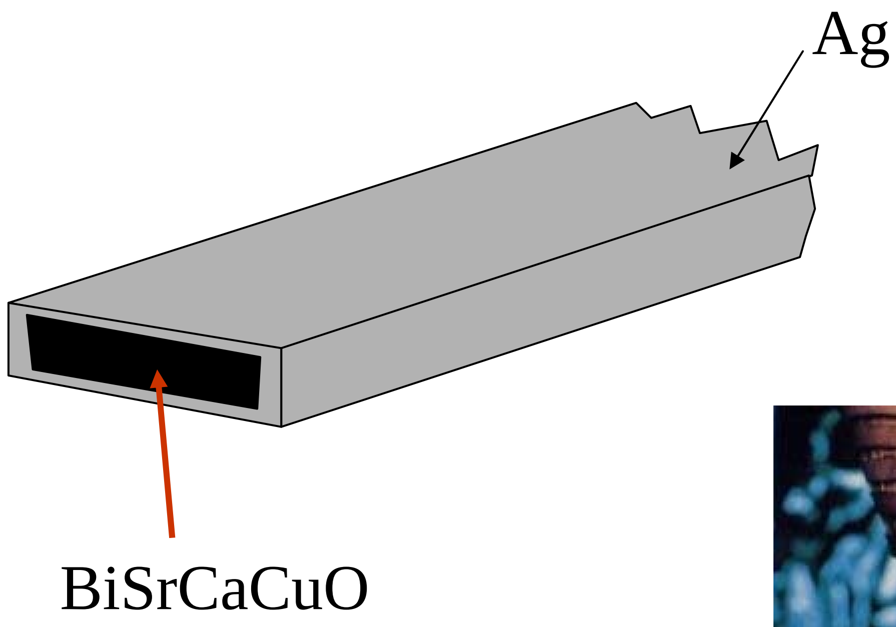

MAGLEV

Benson, p.314

Imagerie par Résonance Magnétique (MRI)

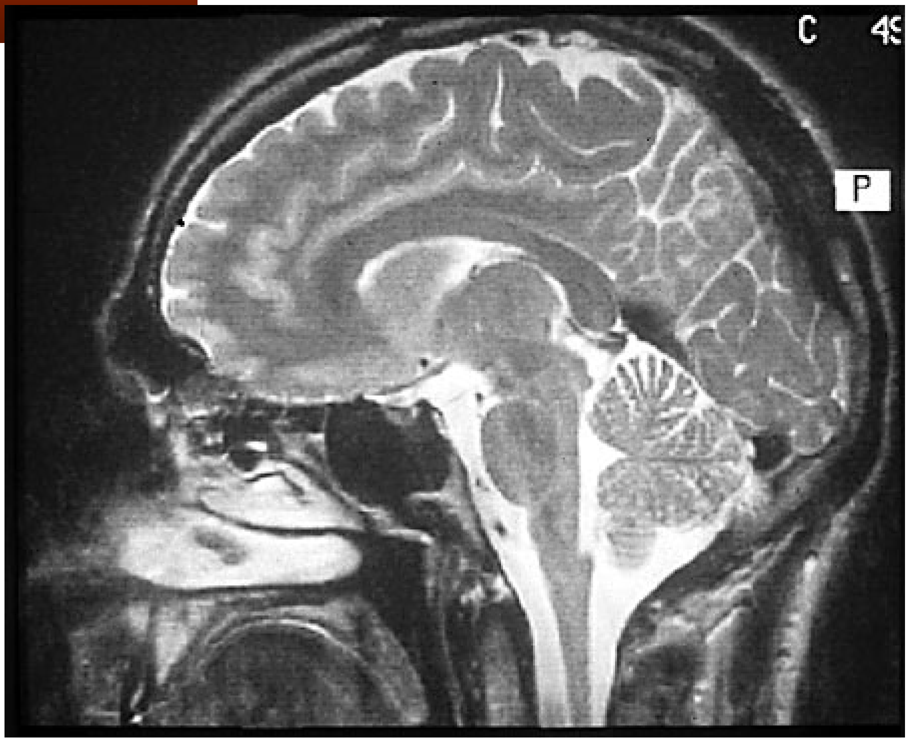

Recherche : 1) Plus hauts champs
2) Autre façon de détecter (SQUID)

Toujours d’actualité !

Vol 447 | 31 May 2007 | doi:10.1038/nature05872

nature

LETTERS

Quantum oscillations and the Fermi surface in an underdoped high-T_c superconductor

Nicolas Doiron-Leyraud[1], Cyril Proust[2], David LeBoeuf[1], Julien Levallois[2], Jean-Baptiste Bonnemaison[1], Ruixing Liang[3,4], D. A. Bonn[3,4], W. N. Hardy[3,4] & Louis Taillefer[1,4]

Toujours d’actualité !

nature Vol 445|1 January 2007|doi:10.1038/nature05437

LETTERS

Spin correlations in the electron-doped high-transition-temperature superconductor $Nd_{2-x}Ce_xCuO_{4\pm\delta}$

NATURE|Vol 443|28 September 2006

CONDENSED-MATTER PHYSICS

Coherent questions

David Snoke

Bose–Einstein condensation occurs when many particles enter into the same, coherent quantum state, and is now claimed to occur in various systems of ‘quasiparticles’ in solids. But is it the right term to use here?

nature Vol 443|28 September 2006|doi:10.1038/nature05117

LETTERS

Bose–Einstein condensation of quasi-equilibrium magnons at room temperature under pumping

S. O. Demokritov[1], V. E. Demidov[1], O. Dzyapko[1], G. A. Melkov[2], A. A. Serga[3], B. Hillebrands[3] & A. N. Slavin[4]

NATURE|Vol 444|14 December 2006

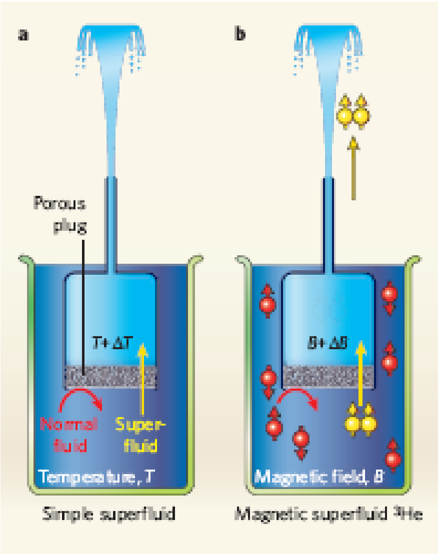

Figure 1 | The magnetic fountain effect. **a**, A simple bosonic superfluid (^4He, for example) comprises a condensed superfluid component mixed into the normal fluid state. When a temperature gradient ΔT is applied across a flow restriction such as a porous plug (a ‘superleak’), the superfluid component flows up through the restriction to equalize the temperature, whereas the normal-fluid component is prevented from passing by its viscosity. The result is a ‘fountain’ of superfluid. **b**, In ^3He, the superfluid component consists of pairs of atoms (yellow), because the fermionic nature of ^3He atoms prevents them from condensing singly into a superfluid state. In the A_1 phase of ^3He studied by Yamaguchi *et al.*[1], the superfluid pairs are highly magnetized, with their spins aligned with a high magnetic field, whereas the unpaired atoms (red) are not magnetized. In this case, the magnetized spin pairs will move to equalize a magnetization difference generated by a magnetic field gradient ΔB, thus supplying the driving force for a magnetic fountain.

Toujours d'actualité !

LETTERS

Charge-density-wave origin of cuprate checkerboard visualized by scanning tunnelling microscopy

W. D. WISE[1], M. C. BOYER[1], KAMALESH CHATTERJEE[1], TAKESHI KONDO[1,2*], T. TAKEUCHI[2,3], H. IKUTA[2], YAYU WANG[1*] AND E. W. HUDSON[1†]

[1]Department of Physics, Massachusetts Institute of Technology, Cambridge, Massachusetts 02139, USA
[2]Department of Crystalline Materials Science, Nagoya University, Nagoya 464-8603, Japan
[3]EcoTopia Science Institute, Nagoya University, Nagoya 464-8603, Japan
*Present address: Ames Laboratory and Department of Physics and Astronomy, Iowa State University, Ames, Iowa 50011, USA (T.K.); Department of Physics, Tsinghua University, Beijing 100084, China (Y.W.)
†e-mail: ehudson@mit.edu

Published online: 6 July 2008; doi:10.1038/nphys1021

Toujours d'actualité

NEWSFOCUS

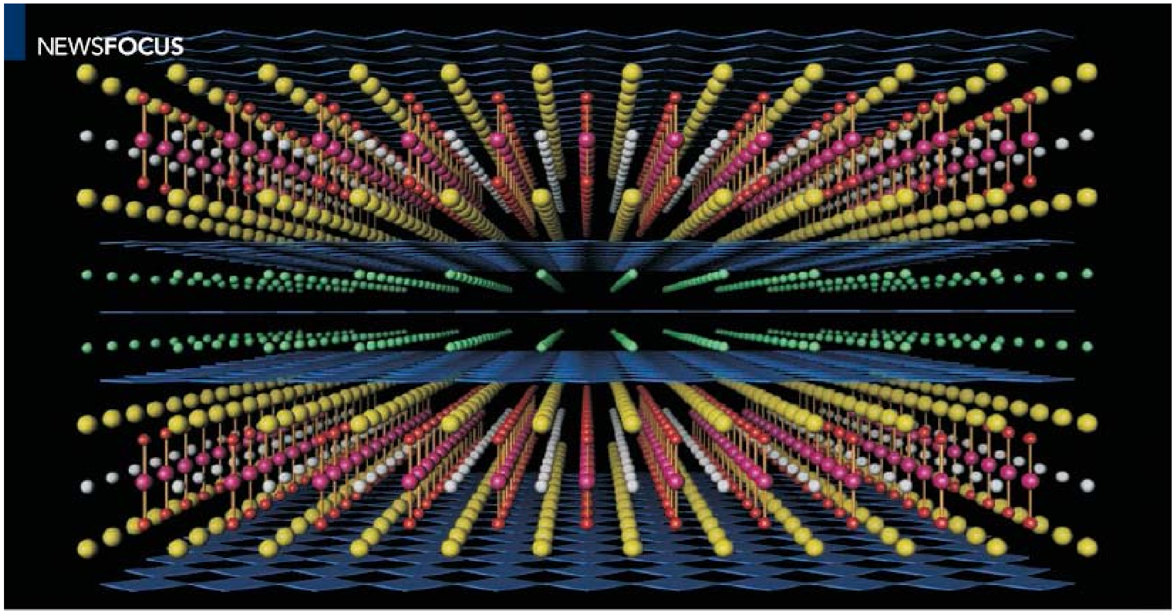

After 2 decades of monumental effort, physicists still cannot explain high-temperature superconductivity. But they may have identified the puzzles they have yet to solve

High T_C: The Mystery That Defies Solution

TWENTY YEARS AGO, A FIRESTORM OF discovery swept through the world of physics. German experimenter J. Georg Bednorz and his Swiss colleague Karl Alexander Müller kindled the flames in September 1986 when they reported that an odd ceramic called lanthanum barium copper oxide carried electricity without any resistance at a temperature of 35 kelvin—12 degrees above the previous record for a superconductor. The blaze ran wild a few months later when Paul Chu of the University of Houston, Texas, and colleagues synthesized yttrium barium copper oxide, a com- giddy enthusiasm. "We had prominent people saying it would all be explained quickly and that we would have superconducting power lines and levitating trains," Ashcroft says.

Ashcroft himself had doubts, however, as he told a class of graduate students a few months later. (I was a member of the class.) The materials comprised four and five elements and possessed elaborate layer-cake structures. They broke the rules about what should make a good superconductor. In short, Ashcroft predicted, high-temperature superconductivity would remain the outstanding 100,000 papers on the materials. Several theorists claim they have deciphered them—although their explanations clash. Still, high-temperature superconductivity has refused to submit to some of the world's best minds.

"The theoretical problem is so hard that there isn't an obvious criterion for *right*," says Steven Kivelson, a theorist at Stanford University in Palo Alto, California. Experimenters are producing a flood of highly detailed data, but physicists struggle to piece the results together, says Joseph Orenstein, an experimenter at the University of California, Berkeley, and Lawrence Berkeley National Laboratory. "It must be close to unique to have so much information and so little consensus on what the questions should be," Orenstein says.

The problem is more than a sliver under the nail. High-temperature superconductivity has shown that physicists' conceptual tools can't handle materials in which electrons shove one another so intensely that it's impossible to disentangle the motion of one from that of the others. Such "strongly correlated" electrons pop up in nanodevices and novel magnets, organic conductors and

M. O. JONES/UNIVERSITY OF OXFORD

UNIVERSITÉ DE SHERBROOKE

Une nouvelle famille de supraconducteurs!

SUPERCONDUCTIVITY

NATURE| Vol 453| 19 June 2008

Prospecting for an iron age

Paul M. Grant

Different material options for high-temperature superconductivity — conduction of electricity with little or no resistance at 'practical' temperatures — have arrived. Iron compounds are the latest thing.

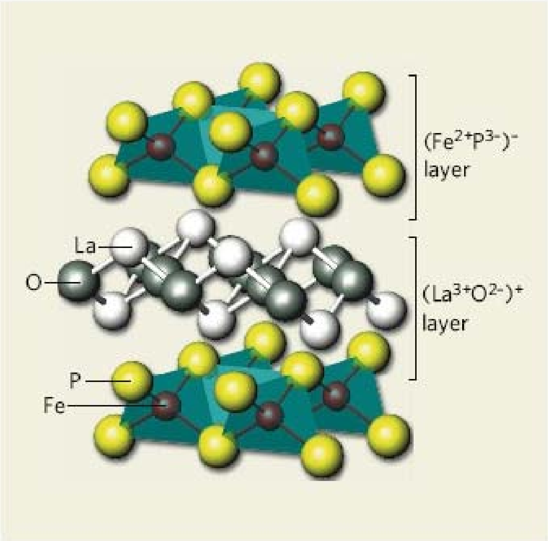

Figure 1 | The unit cell of LaOFeP. In this generic example[3] of the family of lanthanum-series oxyfluoride ferrous pnictides, the overall cell charge is neutral but the individual layers are not, implying electron doping of the FeP layer. Note also that the P coordination of Fe is tetrahedral, not square planar as is the case for the high-T_c copper oxide perovskites. (Reproduced from ref. 3.)

Condensation de Bose Einstein

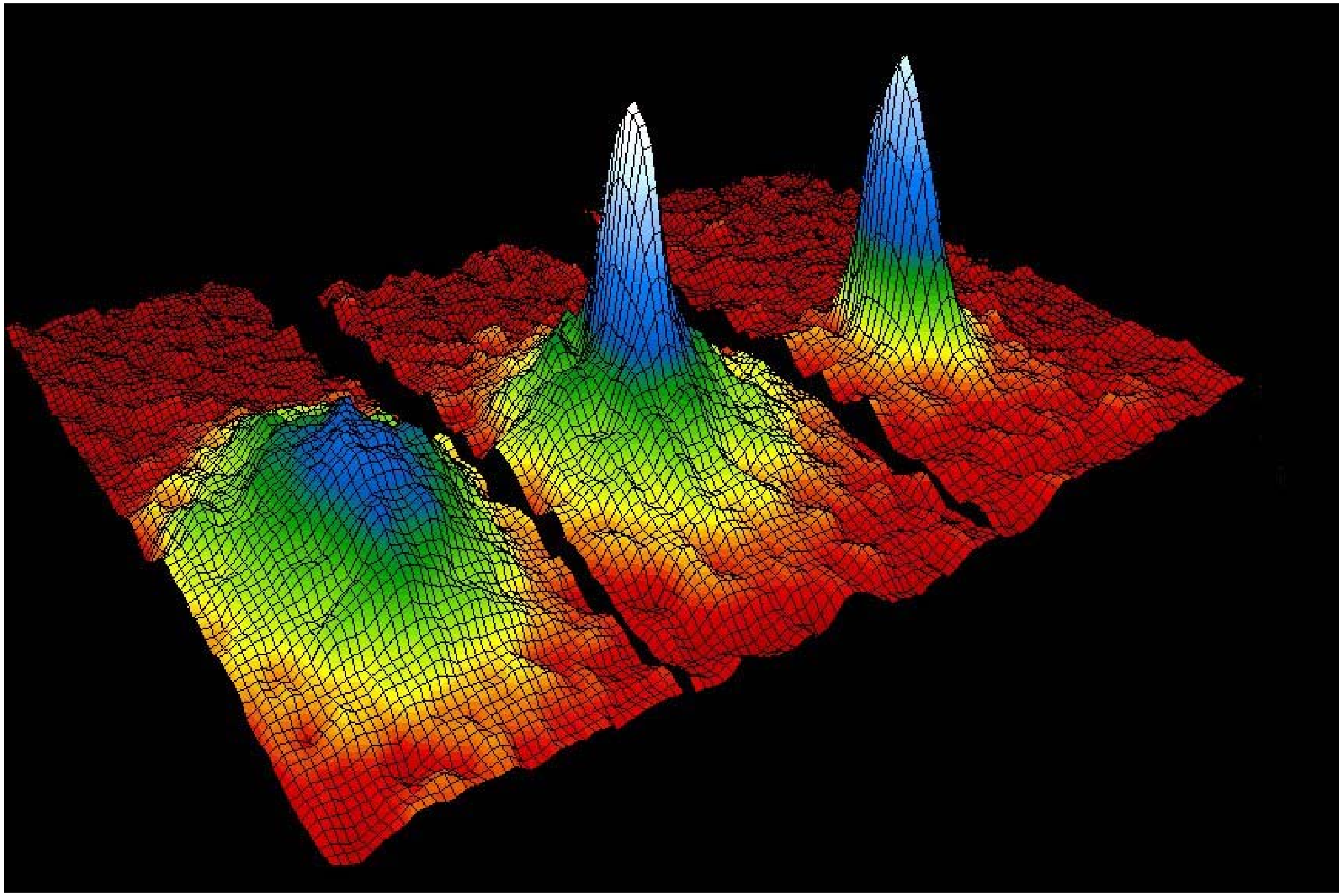

Condensation de Bose Einstein à 400, 200 et 50 nano-Kelvins

Symétries brisées et états cohérents, PHY-740

Diamagnétisme parfait

(Effet Meissner)

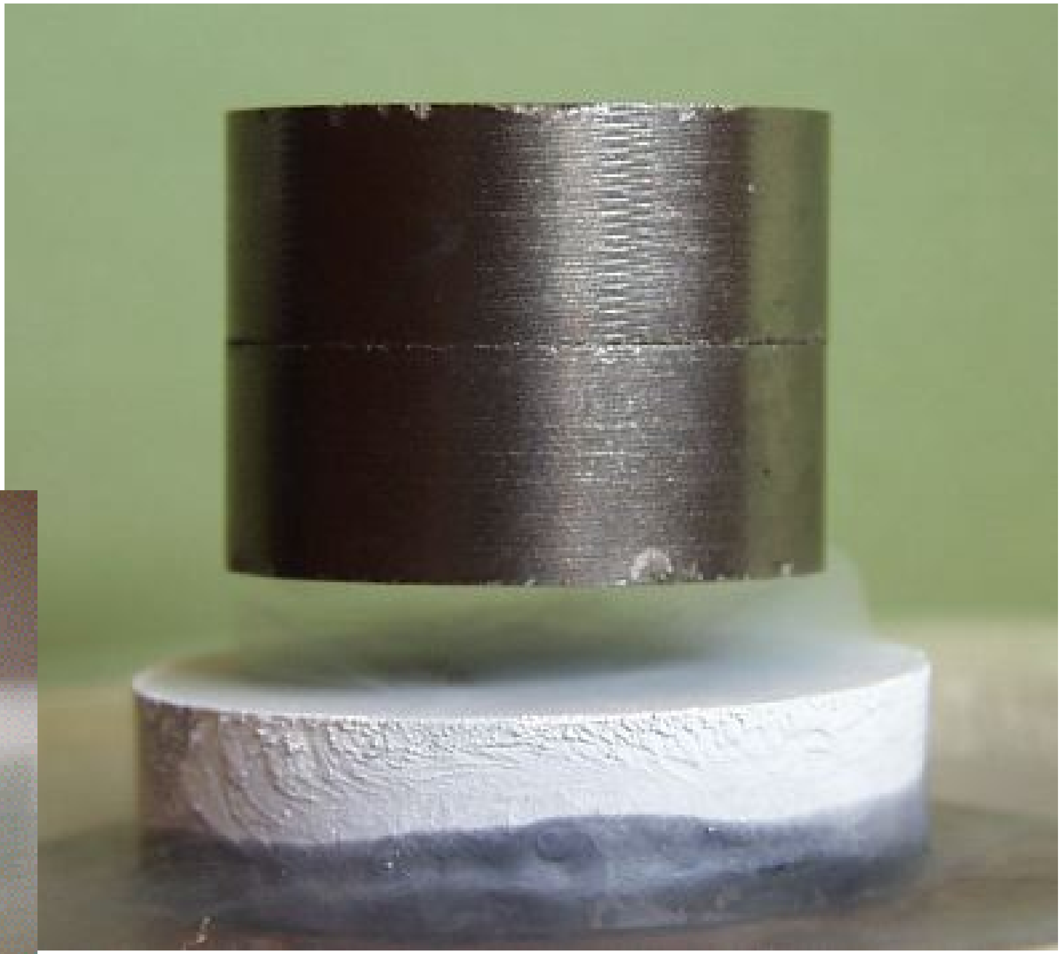

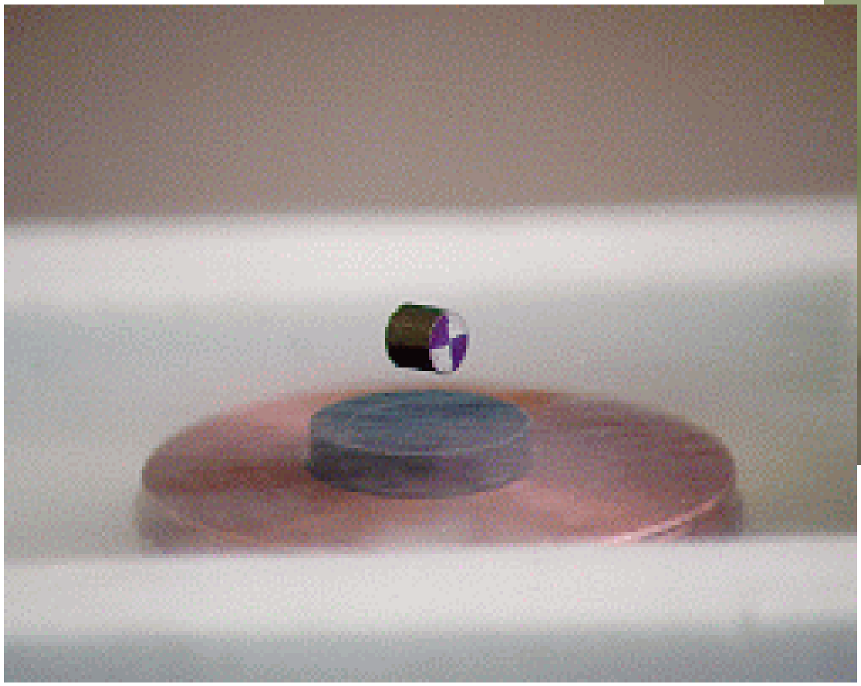

André-Marie Tremblay

UNIVERSITÉ DE SHERBROOKE

Supraconducteurs à haute température

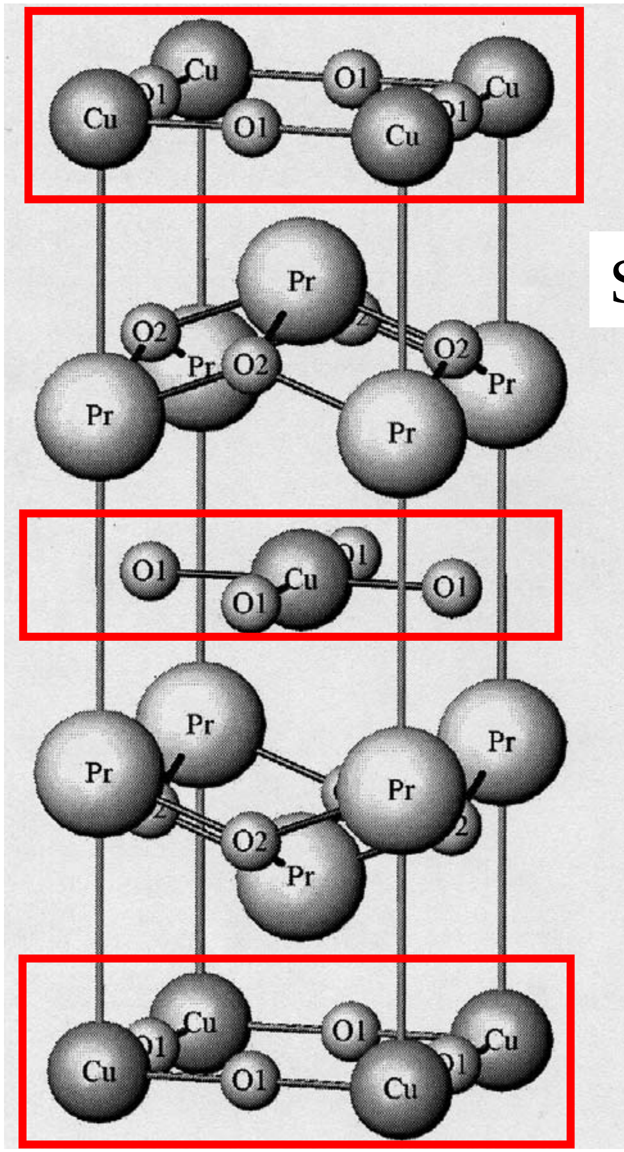

Symétrie brisée, (aussi, cristaux liquides)

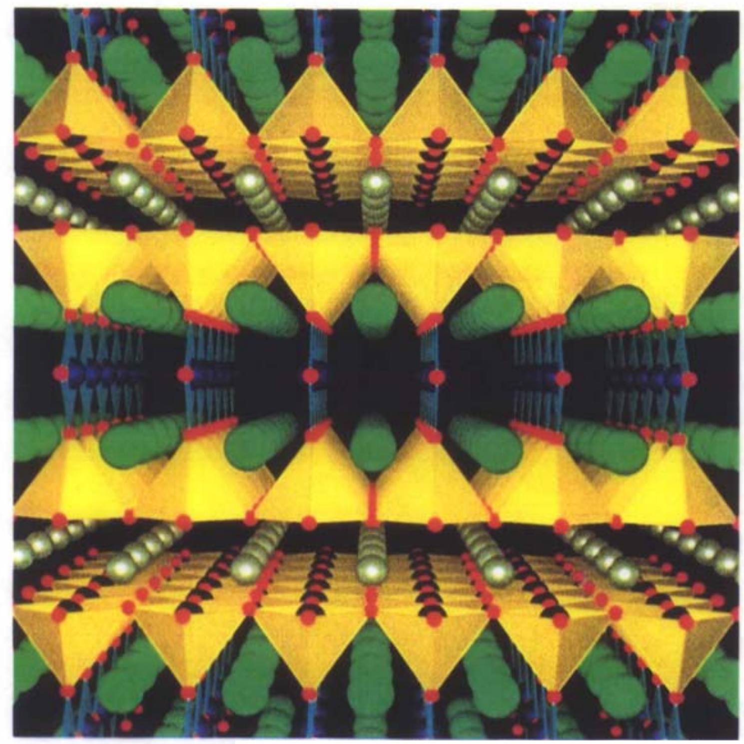

$YBa_2Cu_3O_{7-\delta}$

Diagramme de phase expérimental

Dopés aux électrons Dopés aux trous

AF ?
Pseudogap
Supra
Pt critique
quantique

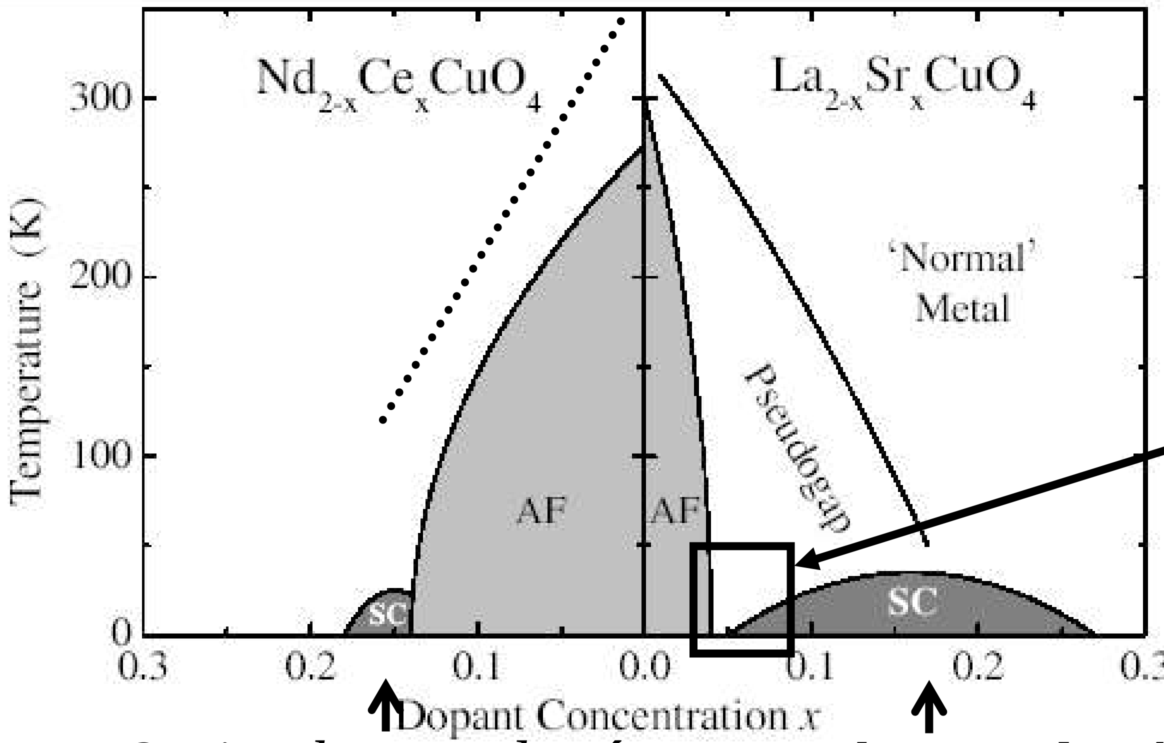

Rayures

Optimalement dopé *Optimalement dopé*

FIG. 1 Phase diagram of n and p-type superconductors.

n, densité électronique

Damascelli, Shen, Hussain, RMP 75, 473 (2003)

Succès et échecs de la théorie des bandes
« Théorie des liquides de Fermi »

n = 1,

Metal selon la théorie des bandes

Isolant antiferromagnétique en réalité

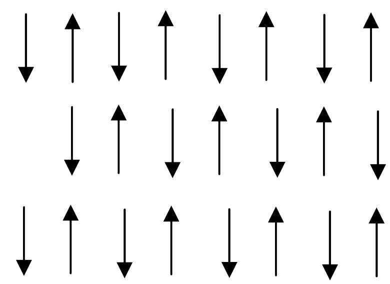

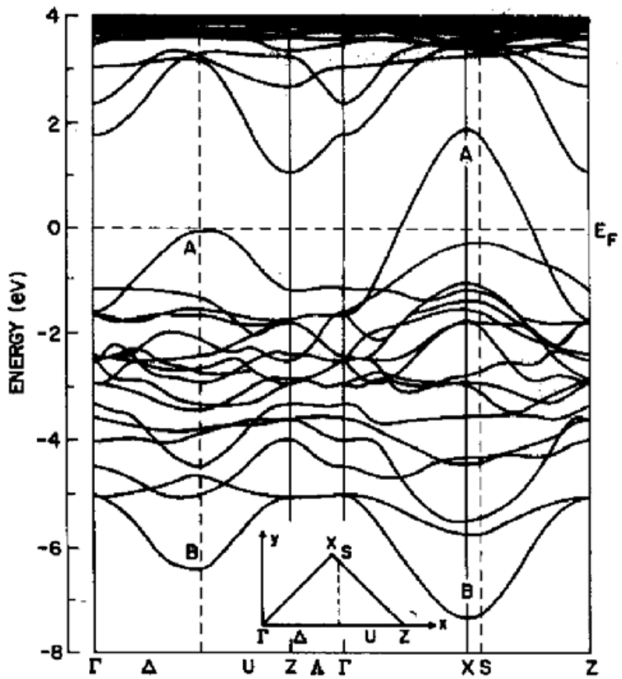

Isolant de Mott…

Chapitre 4 et 6

Ondes de spin: mode collectif, phénomène émergent

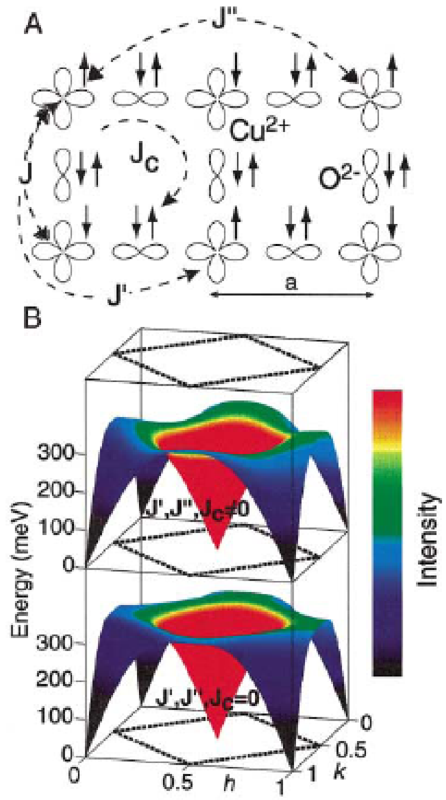

FIG. 1 (color). (A) The CuO_2 plane showing the atomic orbitals (Cu $3d_{x^2-y^2}$ and O $2p_{x,y}$) involved in the magnetic interactions. J, J', and J'' are the first-, second-, and third-nearest-neighbor exchanges and J_c is the cyclic interaction which couples spins at the corners of a square plaquette. Arrows indicate the spins of the valence electrons involved in the exchange. (B) Lower surface is the dispersion relation for $J = 136$ meV and no higher-order magnetic couplings or quantum corrections. The upper surface shows the effect of the higher-order magnetic interactions determined by the present experiment. Color represents spin-wave intensity.

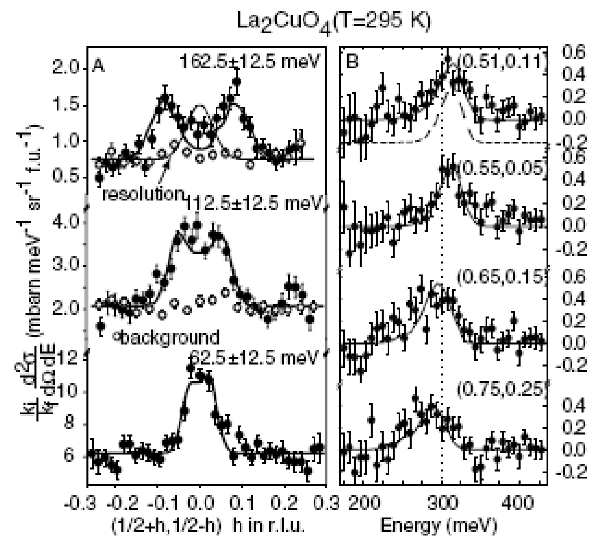

FIG. 2. Scattering from the spin waves in La_2CuO_4 ($T = 295$ K). Data result from 68 h (A) and 98 h (B) counting at a proton current of 170 μA. The sample is described in [10]. Solid lines are fits to a spin-wave cross section convolved with the instrumental resolution. (A) Const-E cuts near the AF zone center for an incident energy $E_i = 250$ meV. Q_z wave vector components at scan centers are $l = 2.8$ (bottom panel), 6.2, and 9.6 r.l.u. of 0.477 Å^{-1}. Open circles are a background measured near the $(0, 0)$ position. Dashed curve is the instrumental response to spin waves of infinite velocity. (B) Const-Q cuts, with $E_i = 750$ meV, yield the dispersion along the AF zone boundary. Vertical dotted line at $E = 300$ meV is a guide to the eye. l values at peak position vary from 8.8 (bottom panel) to 9.5 (top panel). A background measured near the nuclear zone center $(1, 0)$ has been subtracted. Dashed curve is the instrumental response to a dispersionless mode.

spin-wave intensities, in absolute units calibrated using acoustic phonon scattering from the sample.

To understand our results, we consider a Heisenberg Hamiltonian including higher-order couplings [13–16]

$$\mathcal{H} = J \sum S_i \cdot S_j + J' \sum S_i \cdot S_{i'} + J'' \sum S_i \cdot S_{i''}$$

UNIVERSITÉ DE SHERBROOKE

Observation directe des états électroniques en *d=2*

Angle Resolved Photoemission Spectroscopy (ARPES)

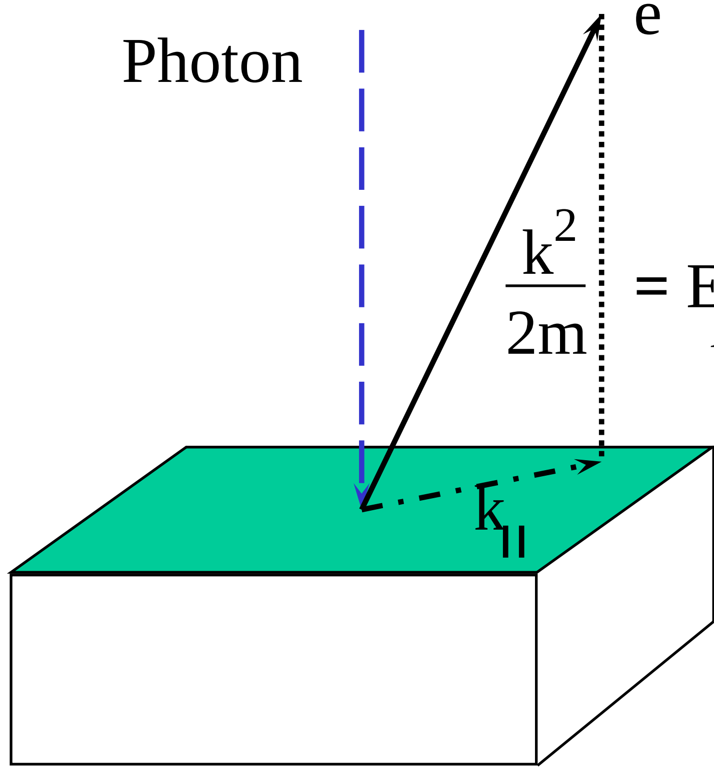

$$\frac{k^2}{2m} = E_{ph} + \omega + \mu - W$$

UNIVERSITÉ DE SHERBROOKE

Radiation synchrotron

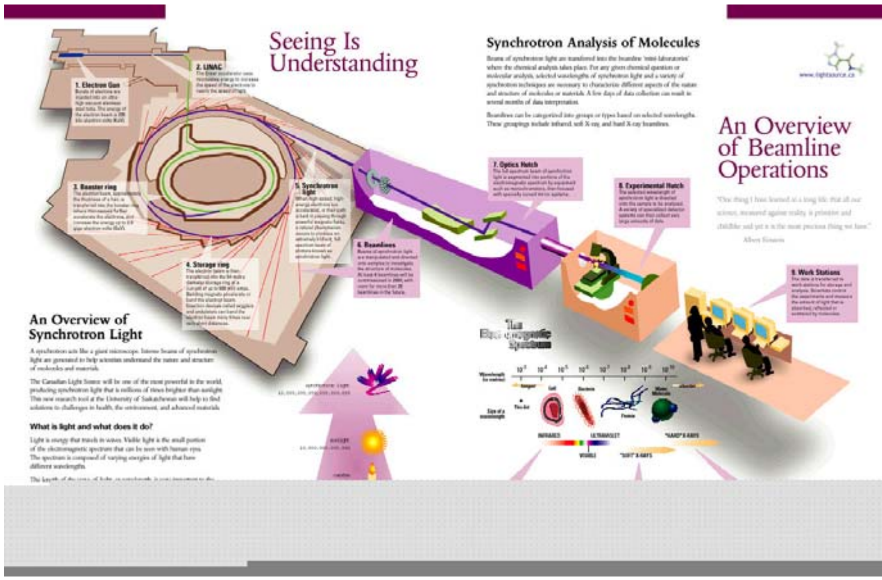

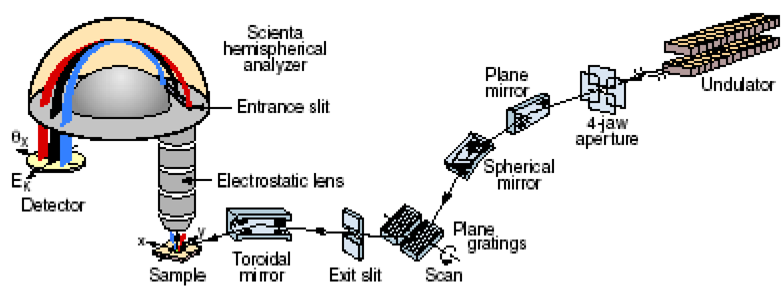

FIG. 6 Generic beamline equipped with a plane grating monochromator and a Scienta spectrometer [Color].

Damascelli, Shen, Hussain, 2002.

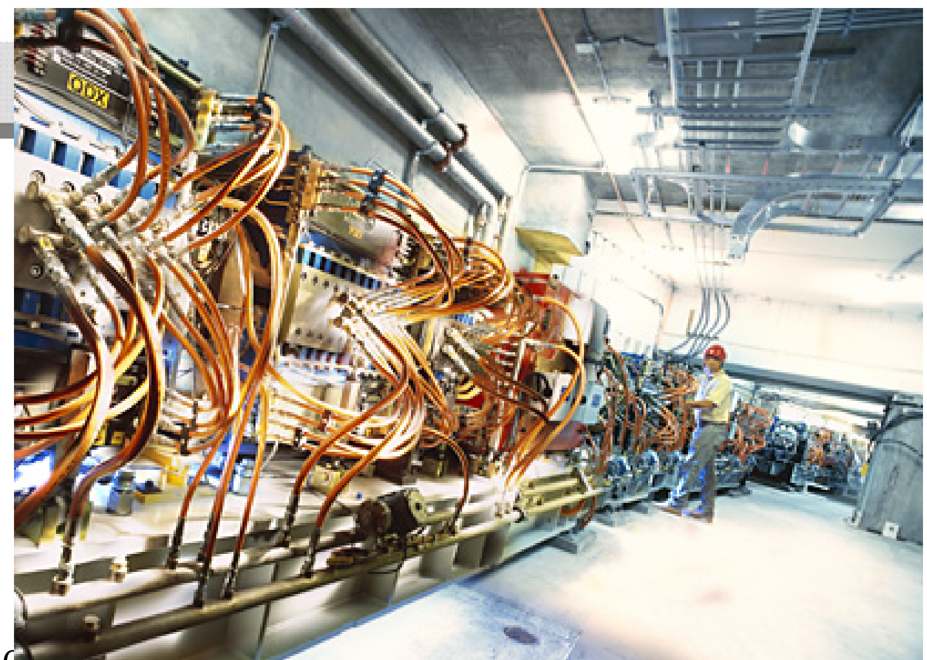

Même l’état « normal » d’un haut Tc n’est pas normal…

Rappel de physique du solide de base

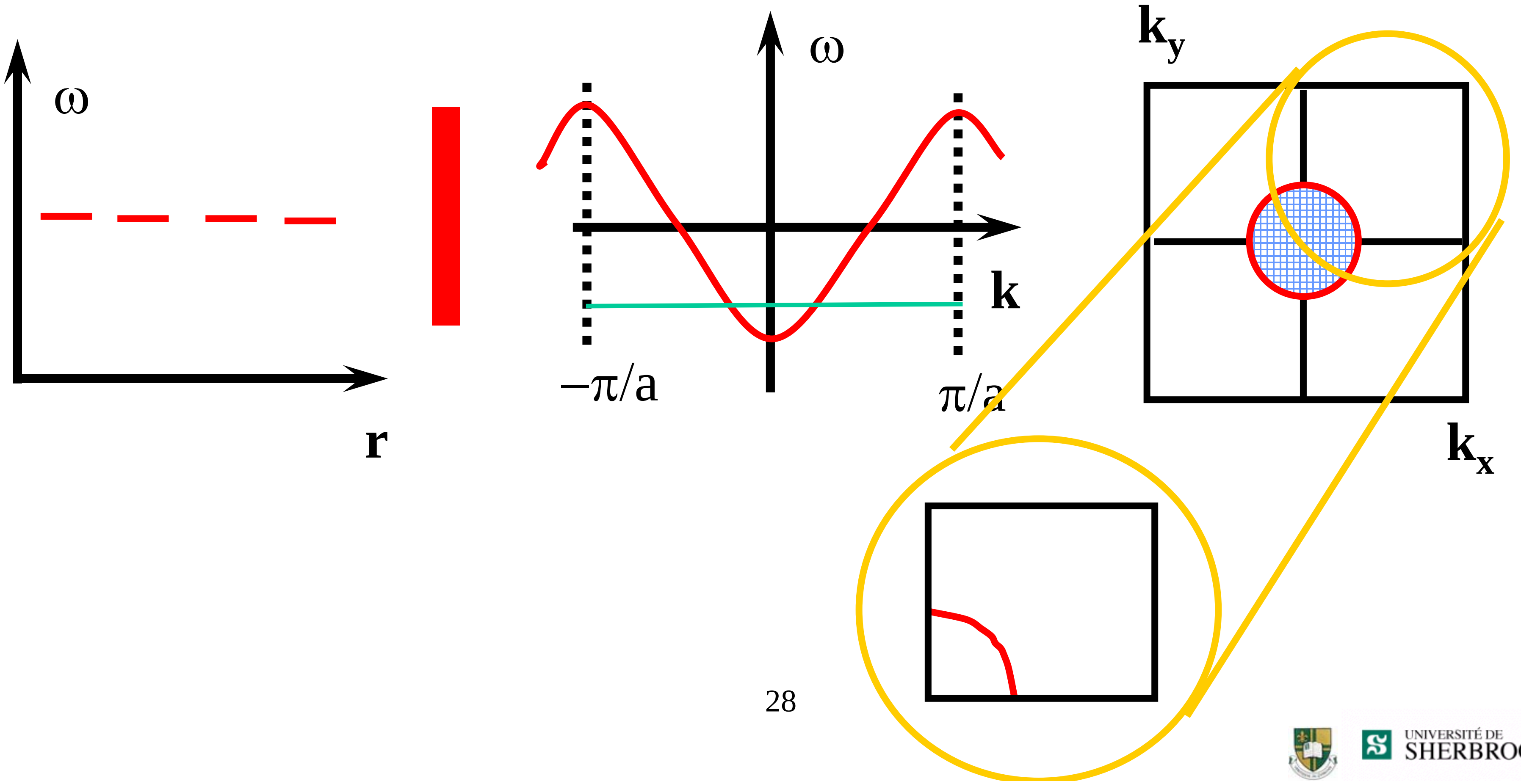

Électrons sans interactions

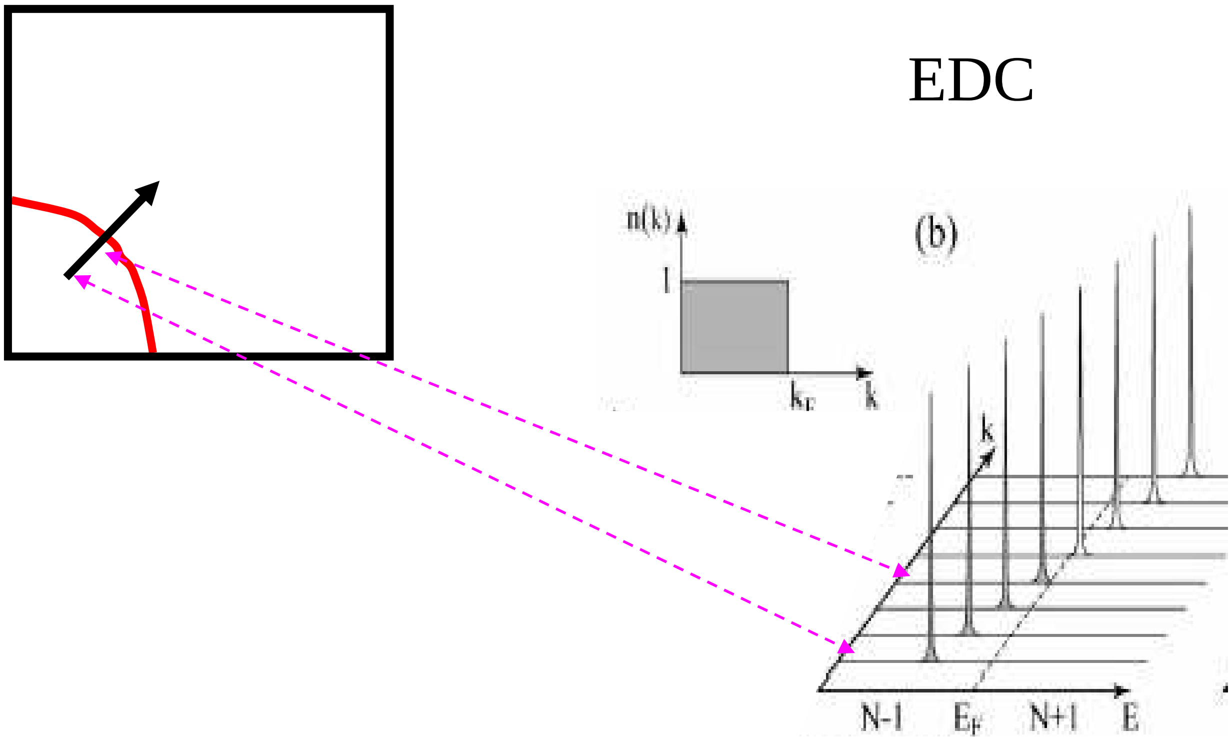

Damascelli, Shen, Hussain, RMP 75, 473 (2003)

Une autre façon de voir les données

MDC

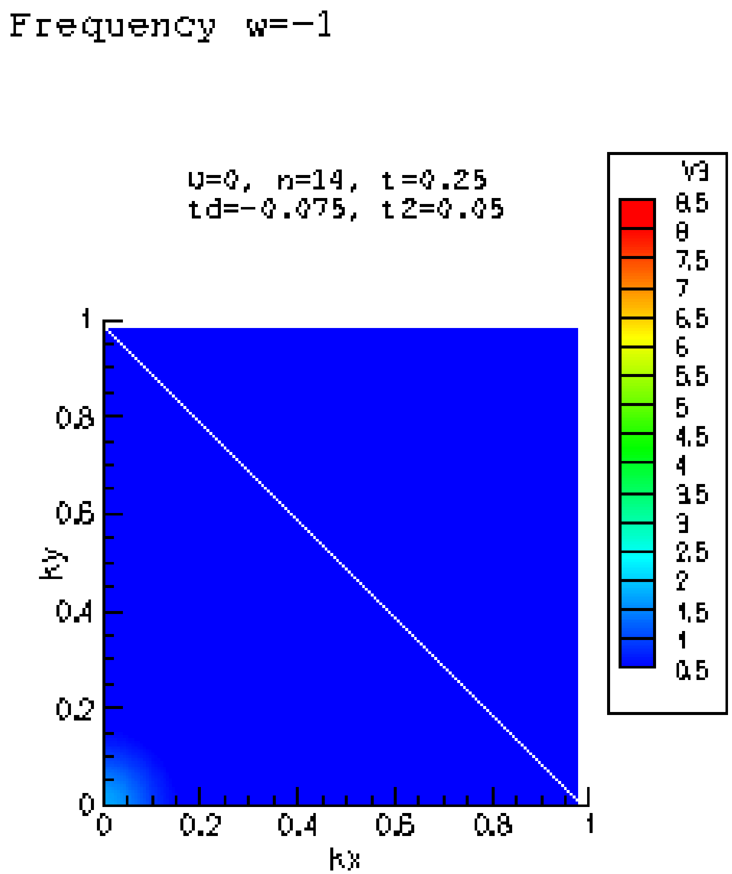

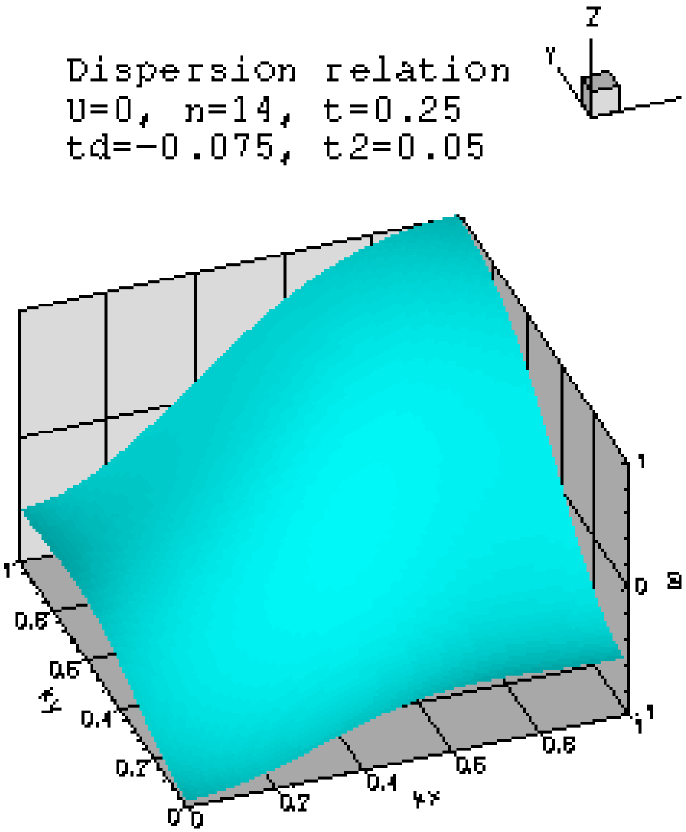

Avec interactions : le liquide de Fermi

A(**k,**ω)*f*(ω)

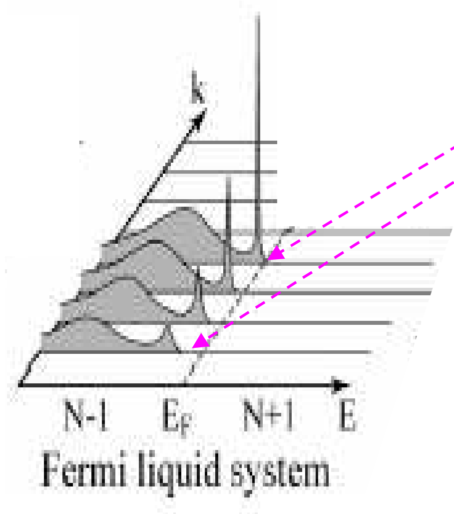

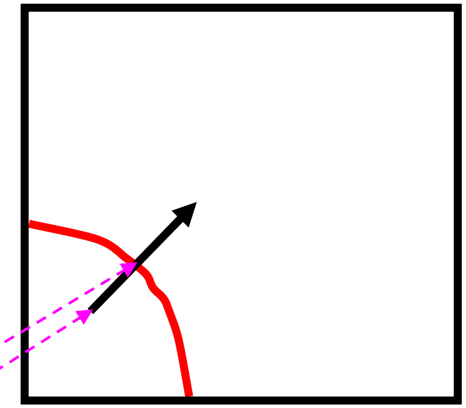

Damascelli, Shen, Hussain, RMP 75, 473 (2003)

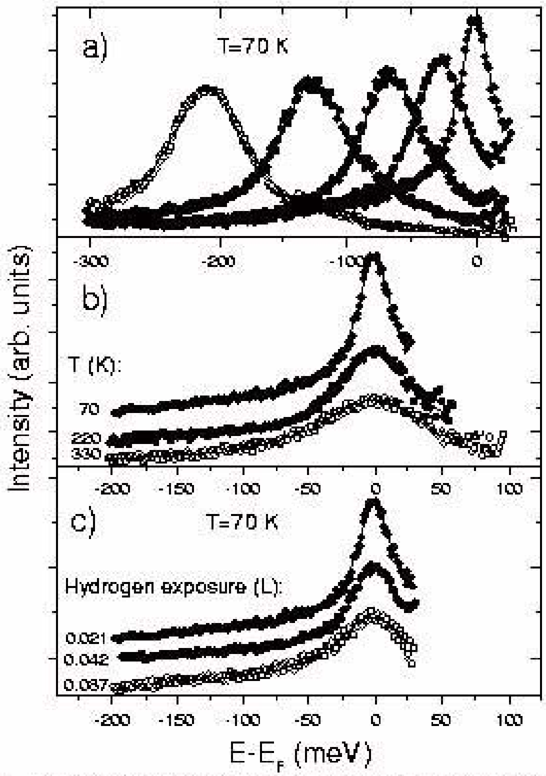

FIG. 2. Spectral intensity as a function of binding energy for constant emission angle, normalized to the experimentally determined Fermi cut-off. Data are symbols, while lines are fits to the Lorentzian peaks with a linear background. The dependence on the binding energy (a), temperature (b), and hydrogen exposure (c) is shown.

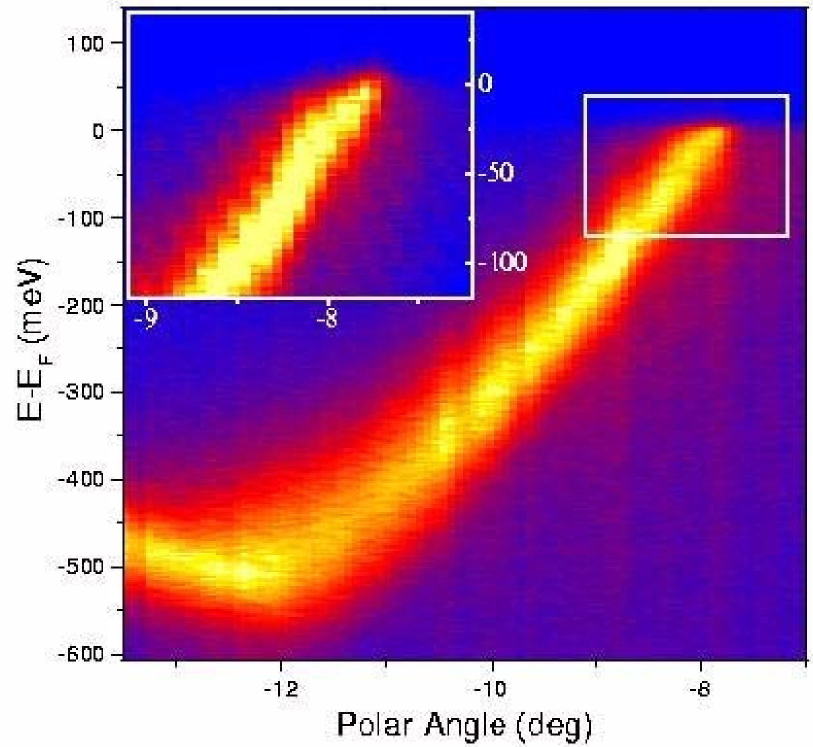

FIG. 1. ARPES intensity plot of the Mo(110) surface recorded along the $\overline{\Gamma}-\overline{\mathrm{N}}$ line of the SBZ at 70 K Shown in the inset is the spectrum of the region around k_F taken with special attention to the surface cleanliness.

T. Valla, A. V. Fedorov, P. D. Johnson, and S. L. Hulbert
P.R.L. **83**, 2085 (1999).

Un liquide de Fermi en *d = 2*

T-$TiTe_2$

$U / W = 0.8$

Perfetti, Grioni et al. Phys. Rev. B **64**, 115102 (2001)

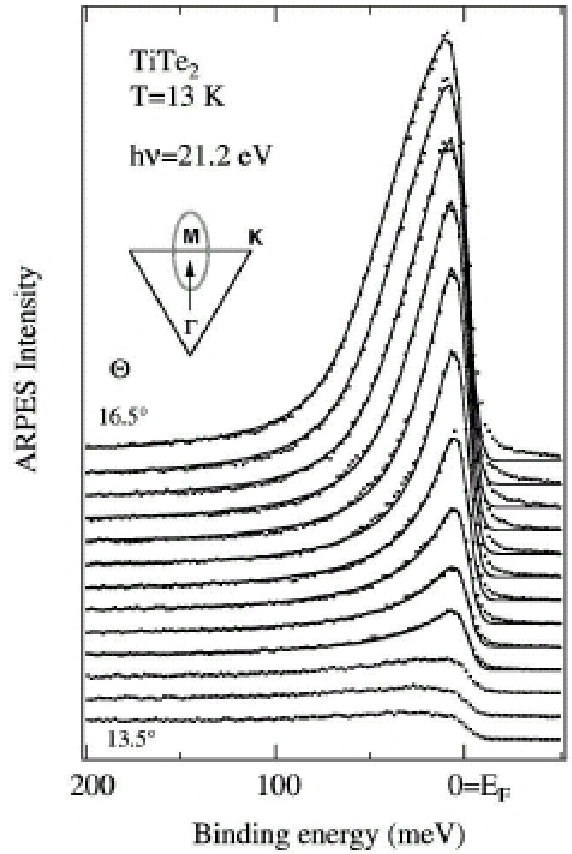

FIG. 1. High-resolution ARPES spectra of 1*T*-$TiTe_2$ measured near the Fermi surface crossing along the high-symmetry Γ*M* direction ($\theta = 0$ is normal emission). The lines are the results of Fermi liquid fits to the data with the parameters discussed in the text. The inset shows a portion of the Brillouin zone with the relevant ellipsoidal electron pocket.

Supraconducteurs

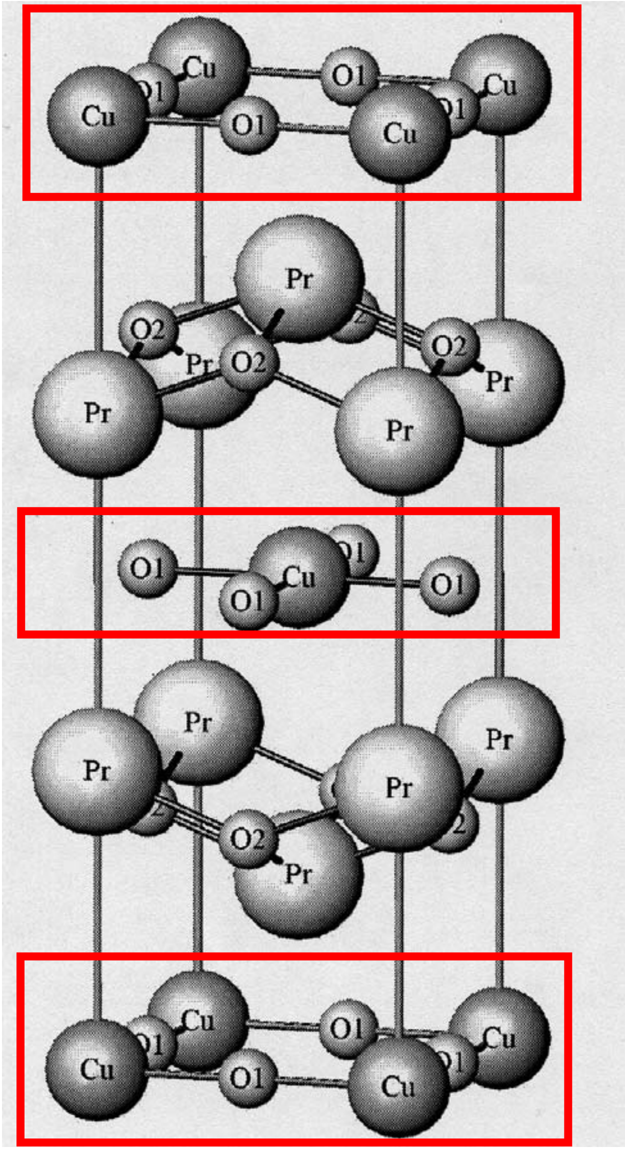

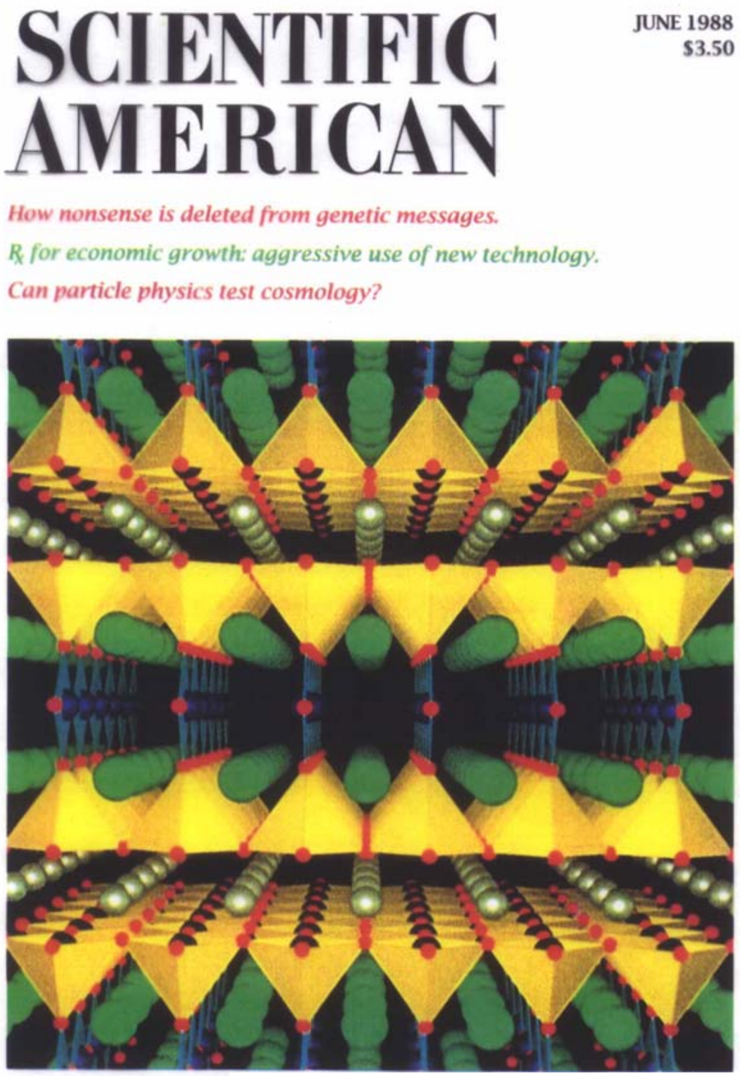

$YBa_2Cu_3O_{7-\delta}$

Surface de Fermi d’un supraconducteur dopé aux électrons

Armitage *et al.* PRL **87**, 147003; **88**, 257001

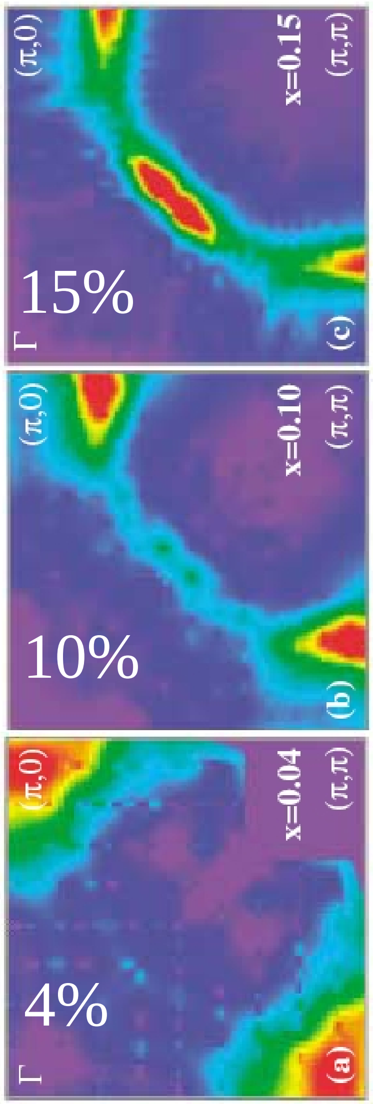

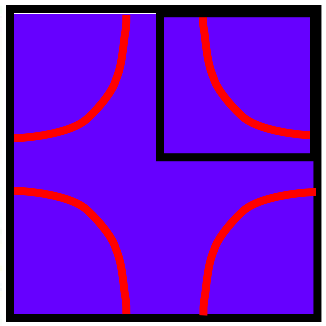

Electron-doped, 17%, *U=8t*

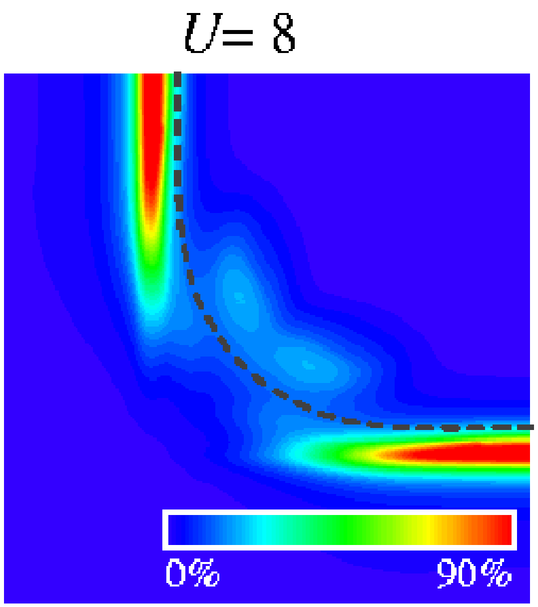

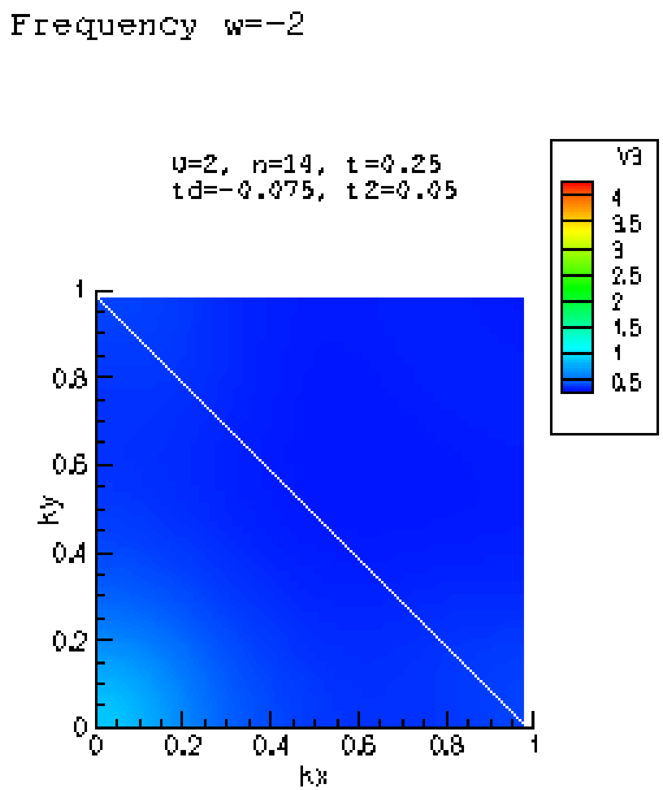

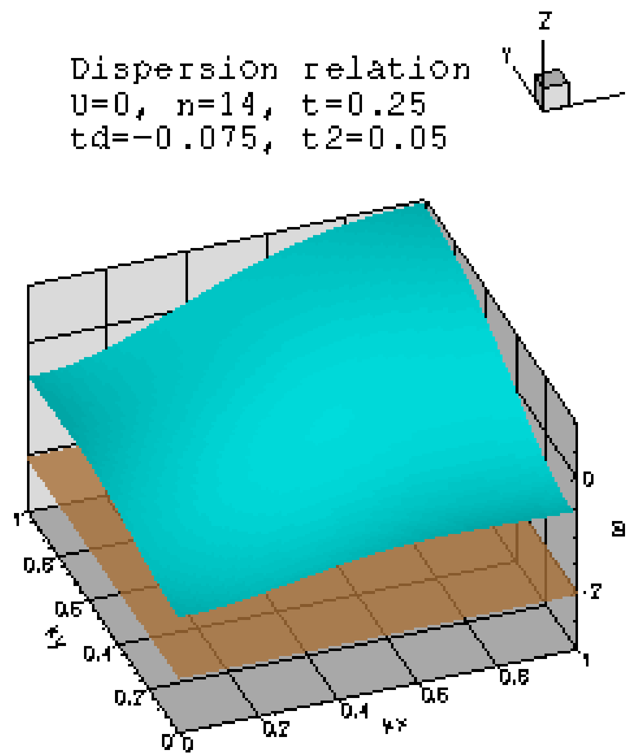

Un modèle d'électrons dans les solides qui décrit magnétisme et supraconductivité?

Modèle de Hubbard à une bande

$$H = \sum_{\sigma} \int \mathrm{d}^3 r \; \psi_\sigma^\dagger(\mathbf{r}) \left(-\frac{\hbar^2}{2m} \nabla^2 + V(\mathbf{r}) \right) \psi_\sigma(\mathbf{r})$$
$$+ \sum_{\sigma,\sigma'} \int \frac{\mathrm{d}^3 r \mathrm{d}^3 r'}{2} U(\mathbf{r}-\mathbf{r}') \psi_\sigma^\dagger(\mathbf{r}) \psi_{\sigma'}^\dagger(\mathbf{r}') \psi_{\sigma'}(\mathbf{r}') \psi_\sigma(\mathbf{r})$$

$$\psi(\mathbf{r}) = \sum_{\mathbf{n}\in\Gamma} c_{\mathbf{n}} w(\mathbf{r}-\mathbf{n})$$

$$H_2 = \frac{1}{4} \sum_{\substack{ijkl \\ \sigma_i\sigma_j\sigma_k\sigma_l}} \langle i\sigma_i, j\sigma_j | U | k\sigma_k, l\sigma_l \rangle c_{i\sigma_i}^\dagger c_{j\sigma_j}^\dagger c_{l\sigma_l} c_{k\sigma_k}$$

Chapitre 5

Échange direct est ferromagnétique !

Un modèle effectif

A. Macridin *et al.*, cond-mat/0411092

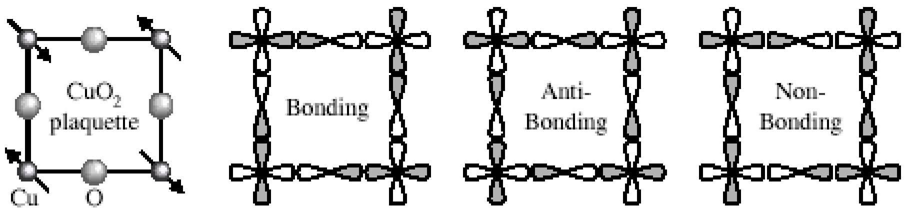

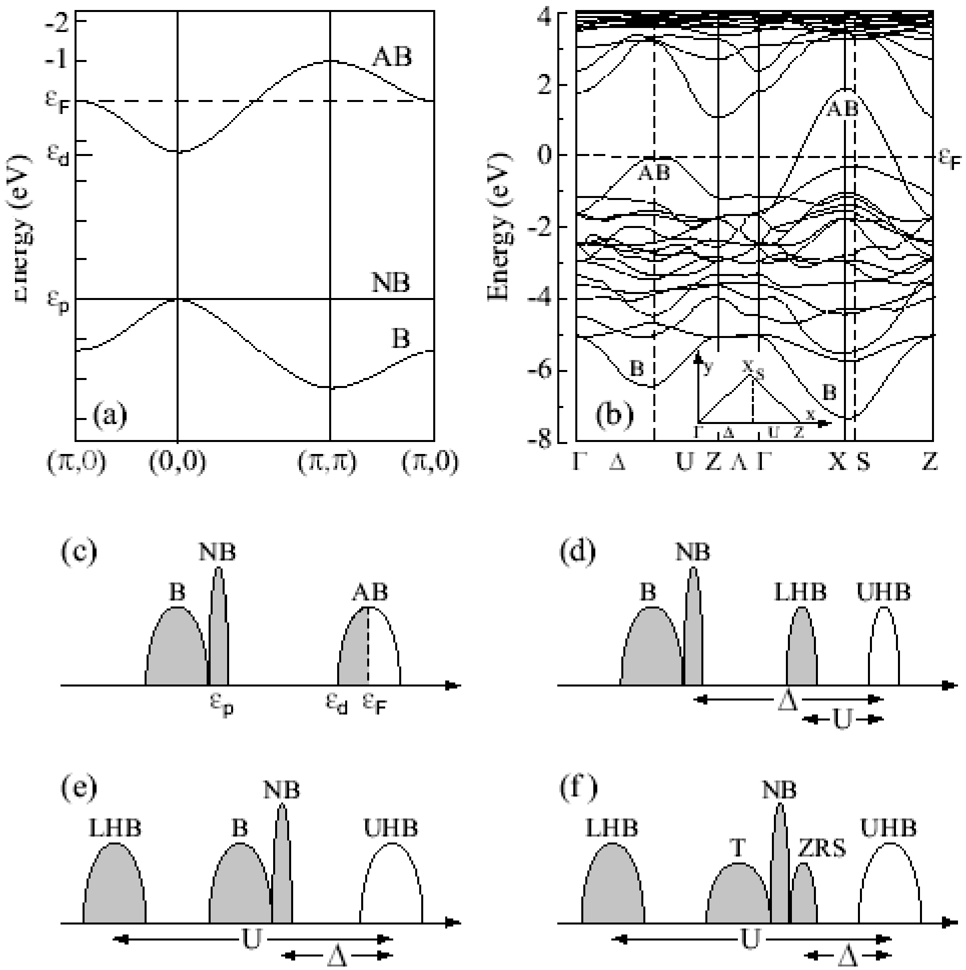

Chapitre 5

Damascelli, Shen, Hussain, RMP 75, 473 (2003)

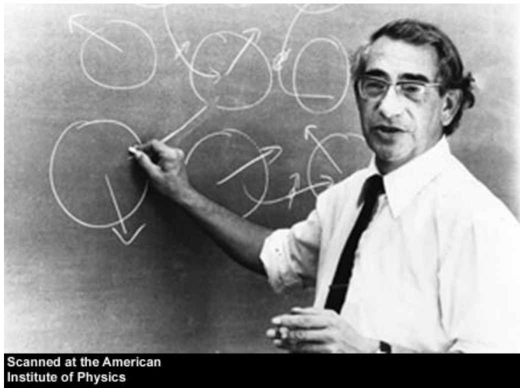

Le modèle de Hubbard

Modèle le plus simple pour les plans
Cu O_2

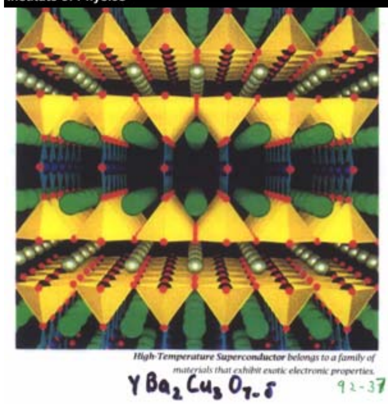

μ

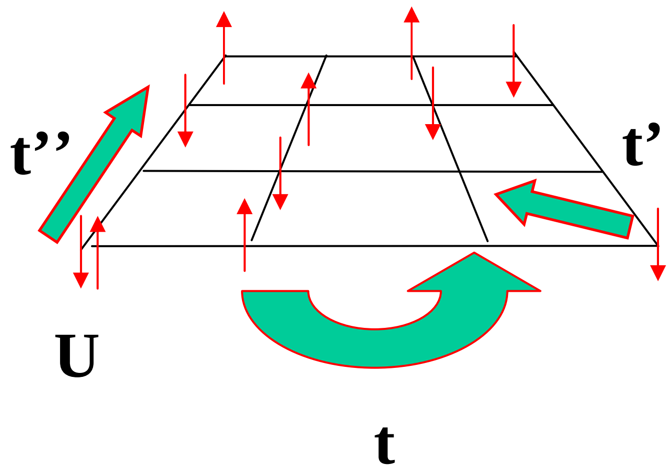

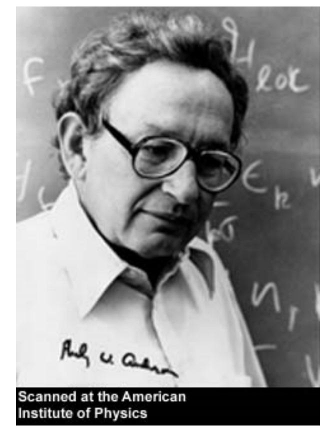

LSCO

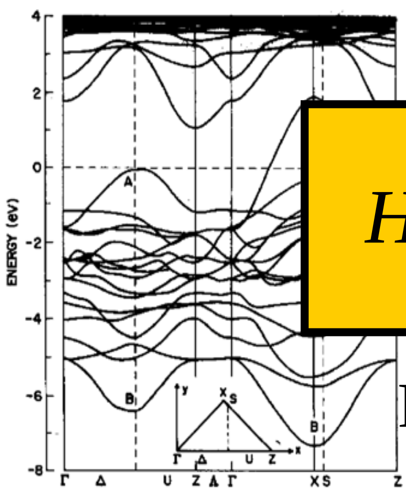

$$H = -\sum_{<ij>\sigma} t_{i,j}\left(c_{i\sigma}^{\dagger}c_{j\sigma} + c_{j\sigma}^{\dagger}c_{i\sigma}\right) + U\sum_i n_{i\uparrow}n_{i\downarrow}$$

Pas de factorisation champ moyen pour supra type d-wave

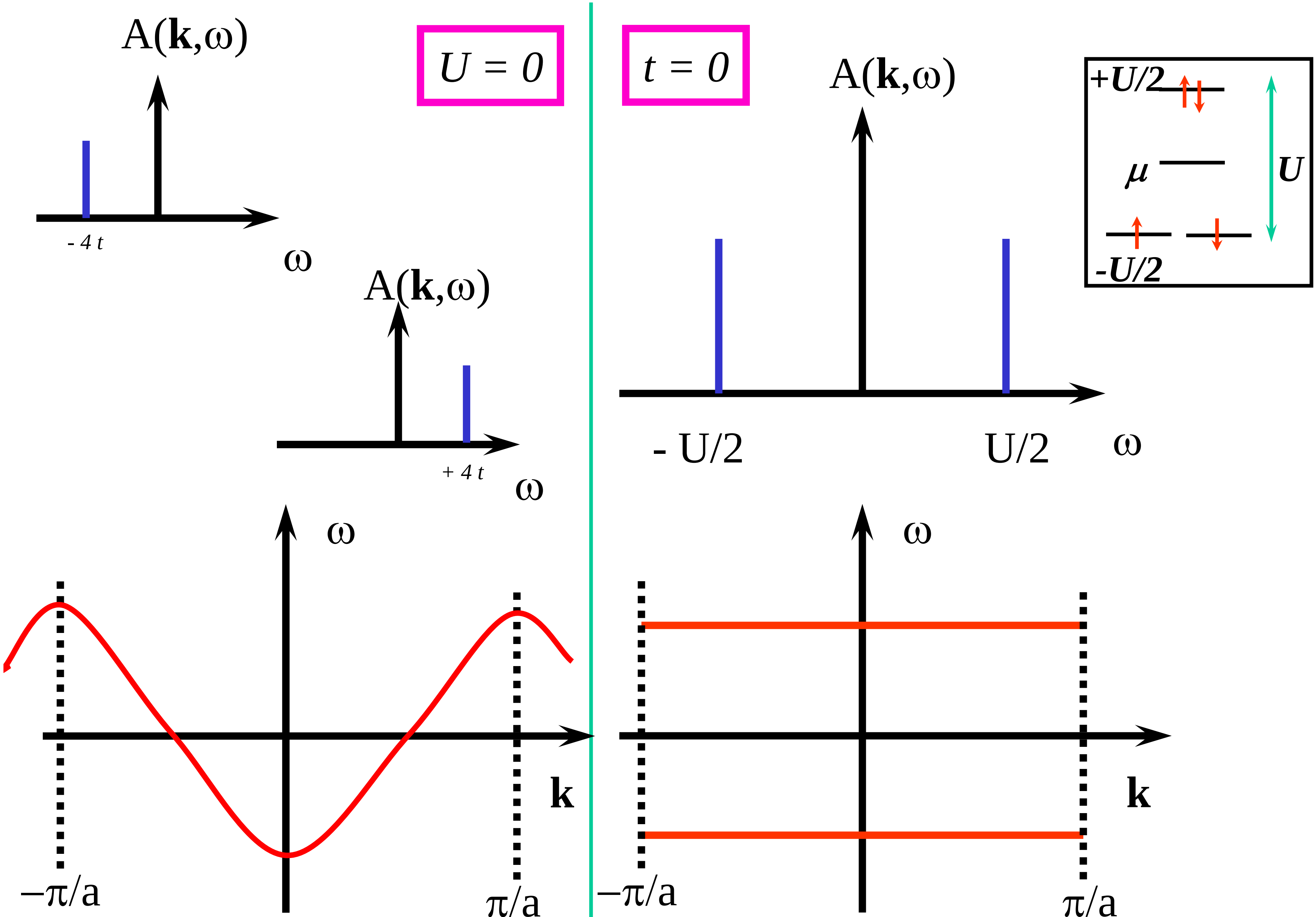
U = 0
A(k,ω)
- 4 t
ω
A(k,ω)
+ 4 t
ω
ω
k
−π/a
π/a
t = 0
A(k,ω)
- U/2
U/2
ω
+U/2
μ
U
-U/2
ω
k
−π/a
π/a

Couplage *faible* vs *fort n=1*

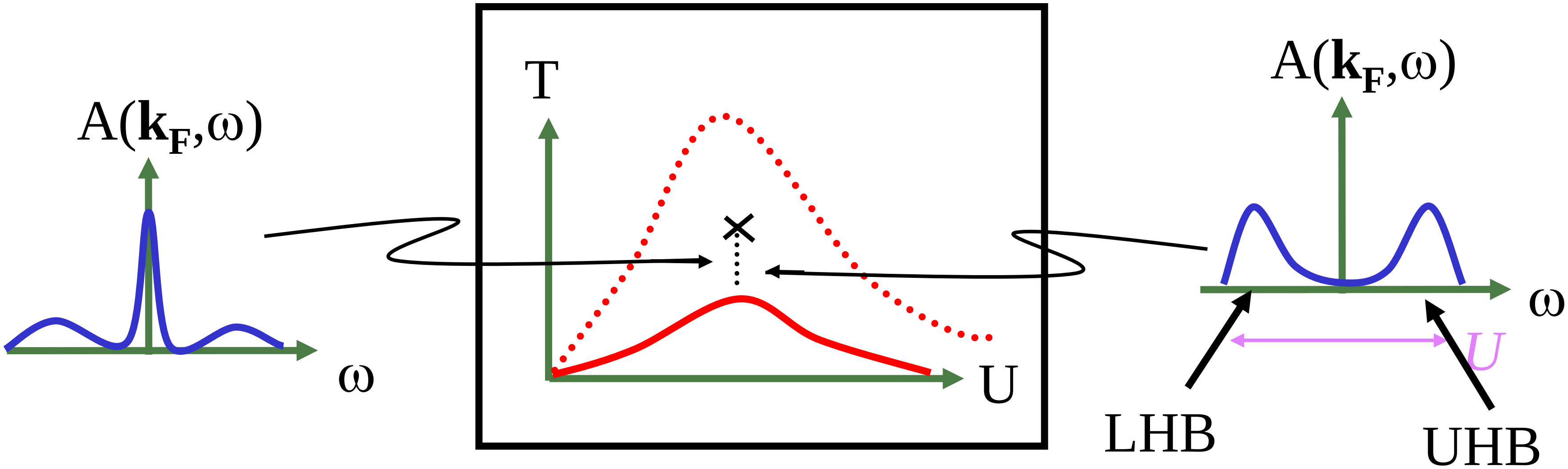

$U \sim 1.5W \quad (W = 8t)$

Transition de Mott

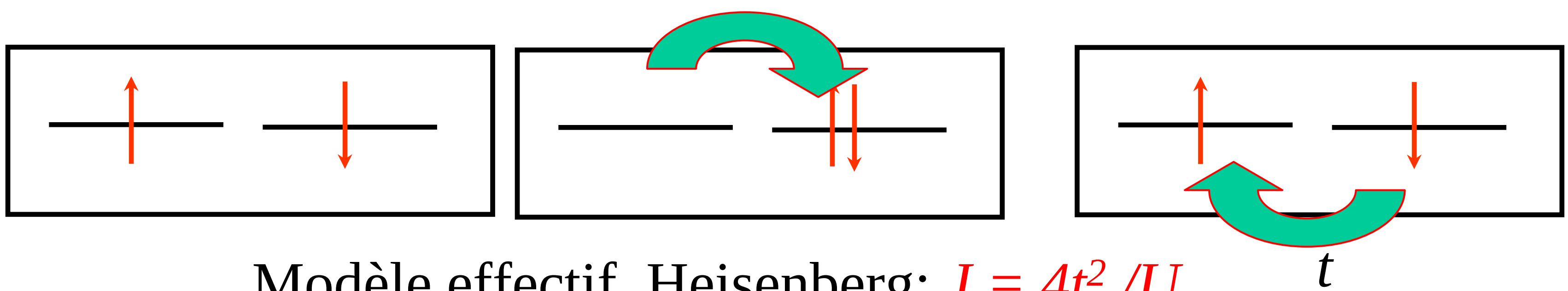

Modèle effectif, Heisenberg: $J = 4t^2/U$

Détruire le liquide de Fermi à demi-rempli
Réseau + interactions

Répulsion forte (transition de Mott)

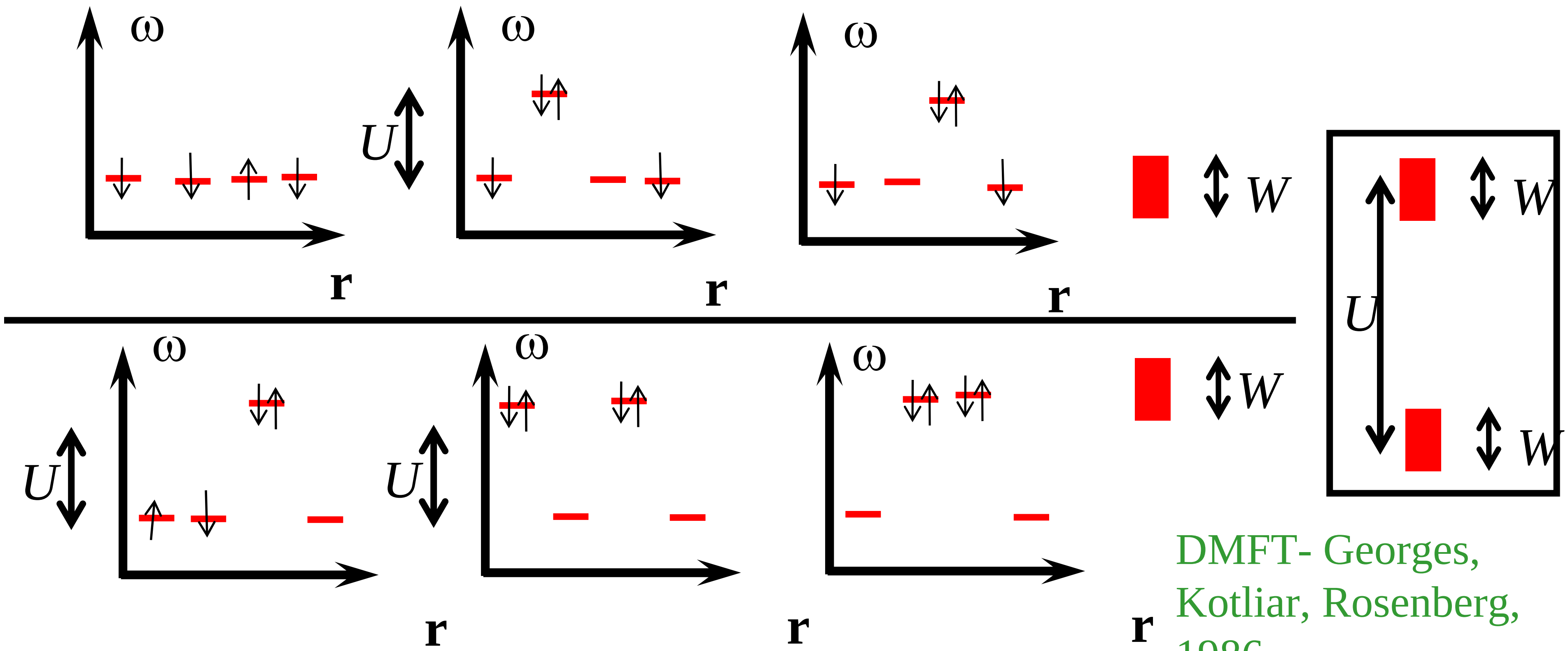

DMFT- Georges, Kotliar, Rosenberg, 1986.

Organiques en couche (famille κ–BEDT-X)

BEDT-TTF layer

Anion layer

(*t'* / *t*)

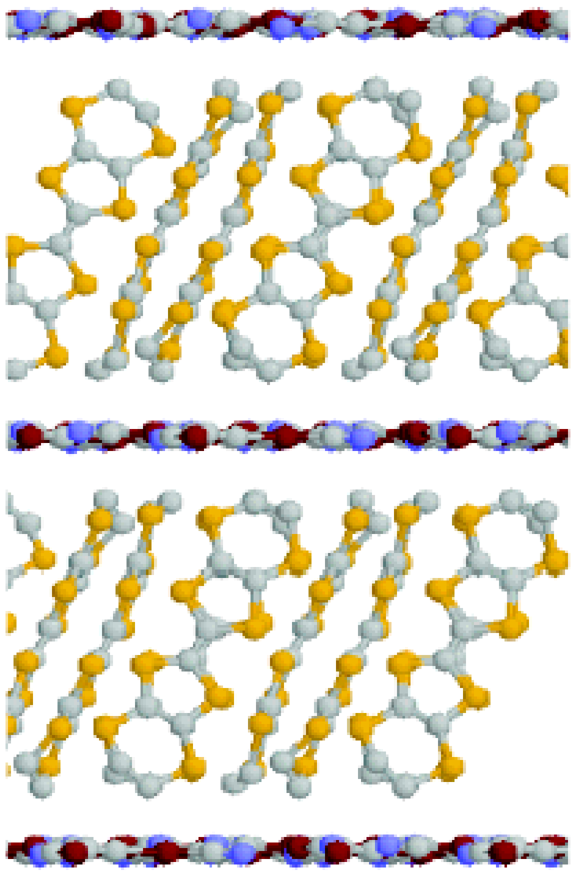

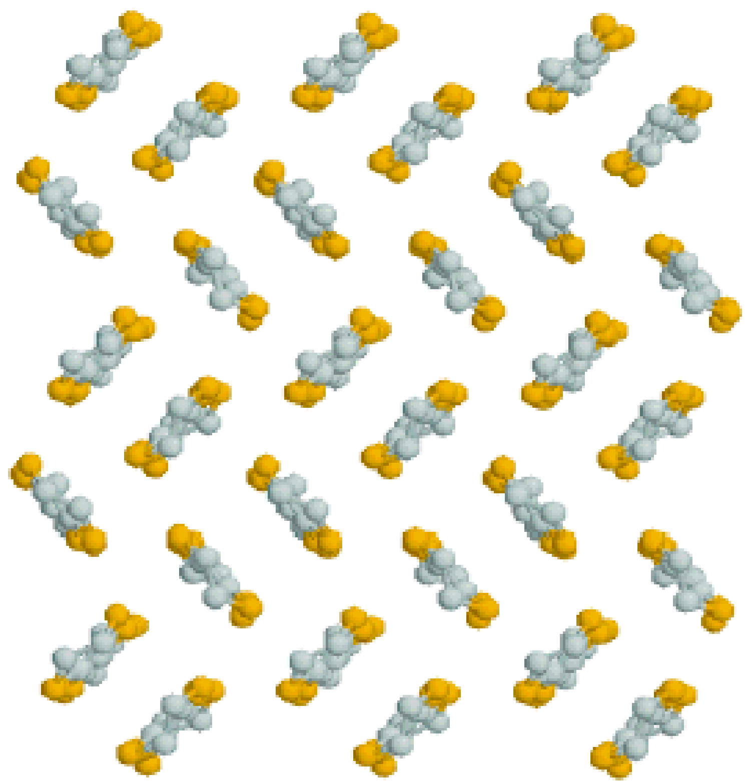

n = *1*

Modèle de Hubbard à une bande pour les organiques

H. Kino + H. Fukuyama, J. Phys. Soc. Jpn **65** 2158 (1996),
R.H. McKenzie, Comments Condens Mat Phys. **18**, 309 (1998)

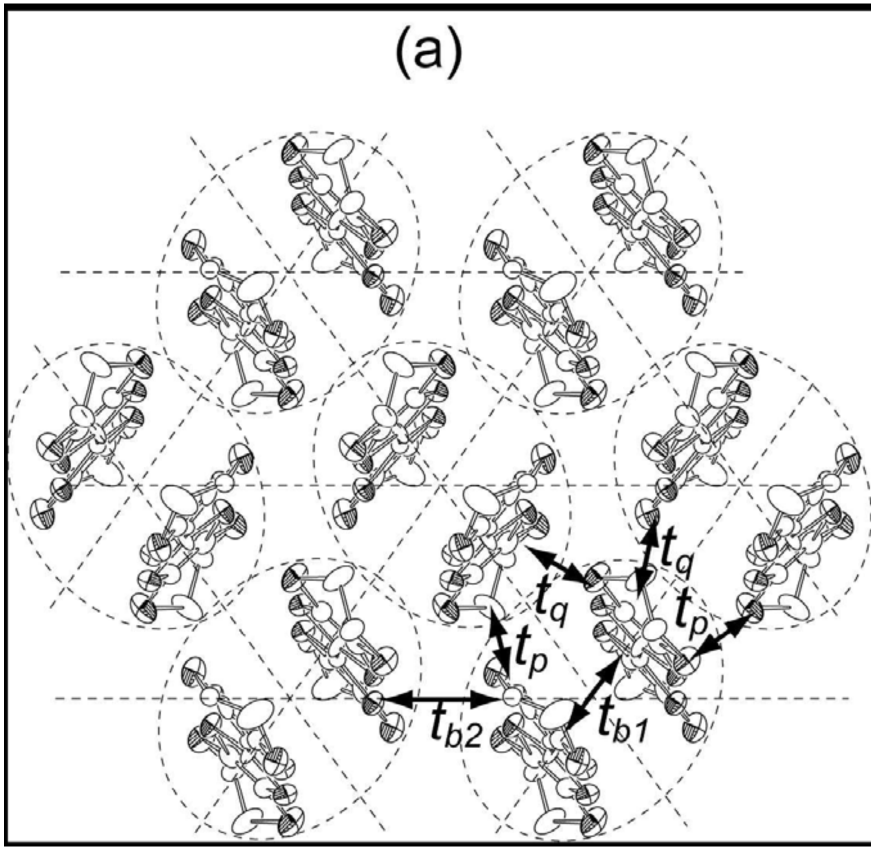

Y. Shimizu, et al. Phys. Rev. Lett. **91**, 107001(2003)

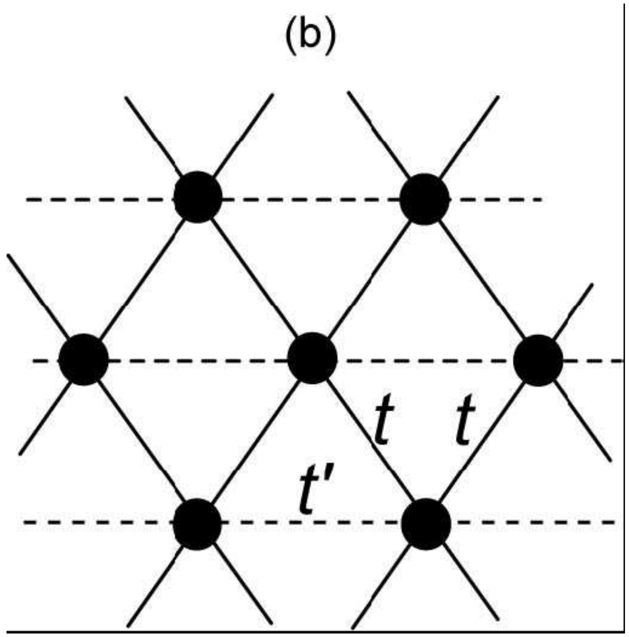

$$t \approx 50\,\mathrm{meV}$$

$$\Rightarrow U \approx 400\,\mathrm{meV}$$

$$t'/t \sim 0.6 - 1.1$$

Diagramme de phase expérimental pour Cl

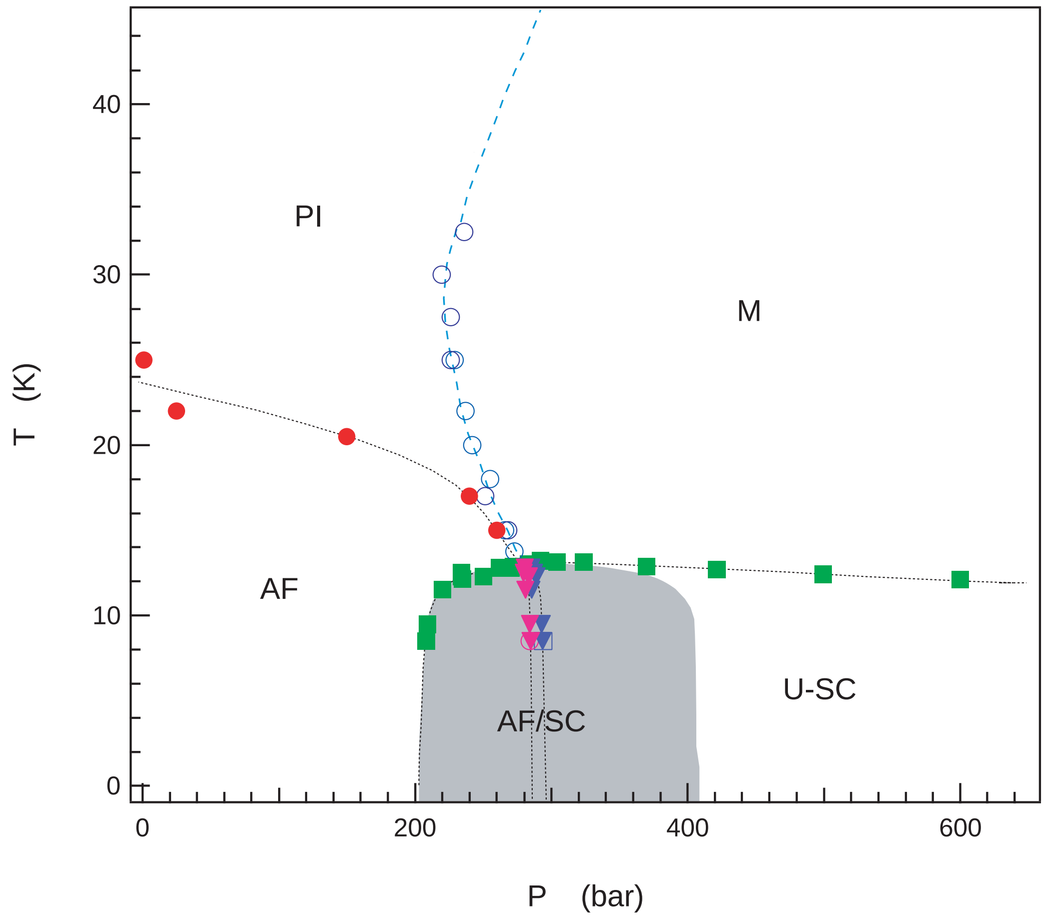

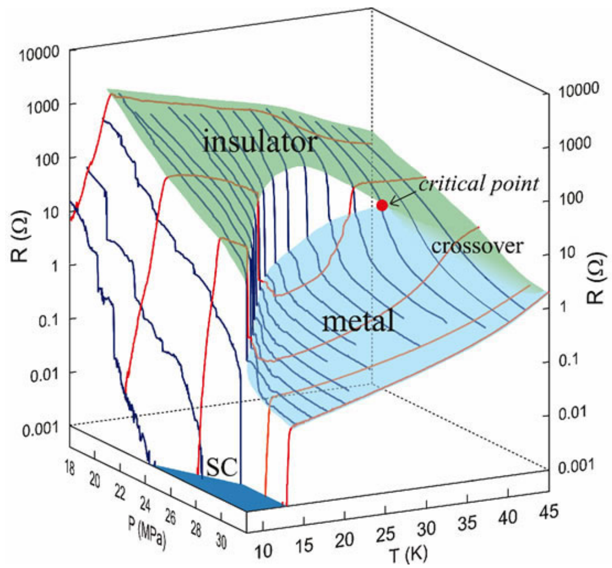

F. Kagawa, K. Miyagawa, + K. Kanoda PRB **69** (2004) +Nature **436** (2005)

Diagramme de phase expérimental (X=Cu[N(CN)$_2$]Cl)

S. Lefebvre et al. PRL **85**, 5420 (2000), P. Limelette, et al. PRL 91 (2003)

Perspective

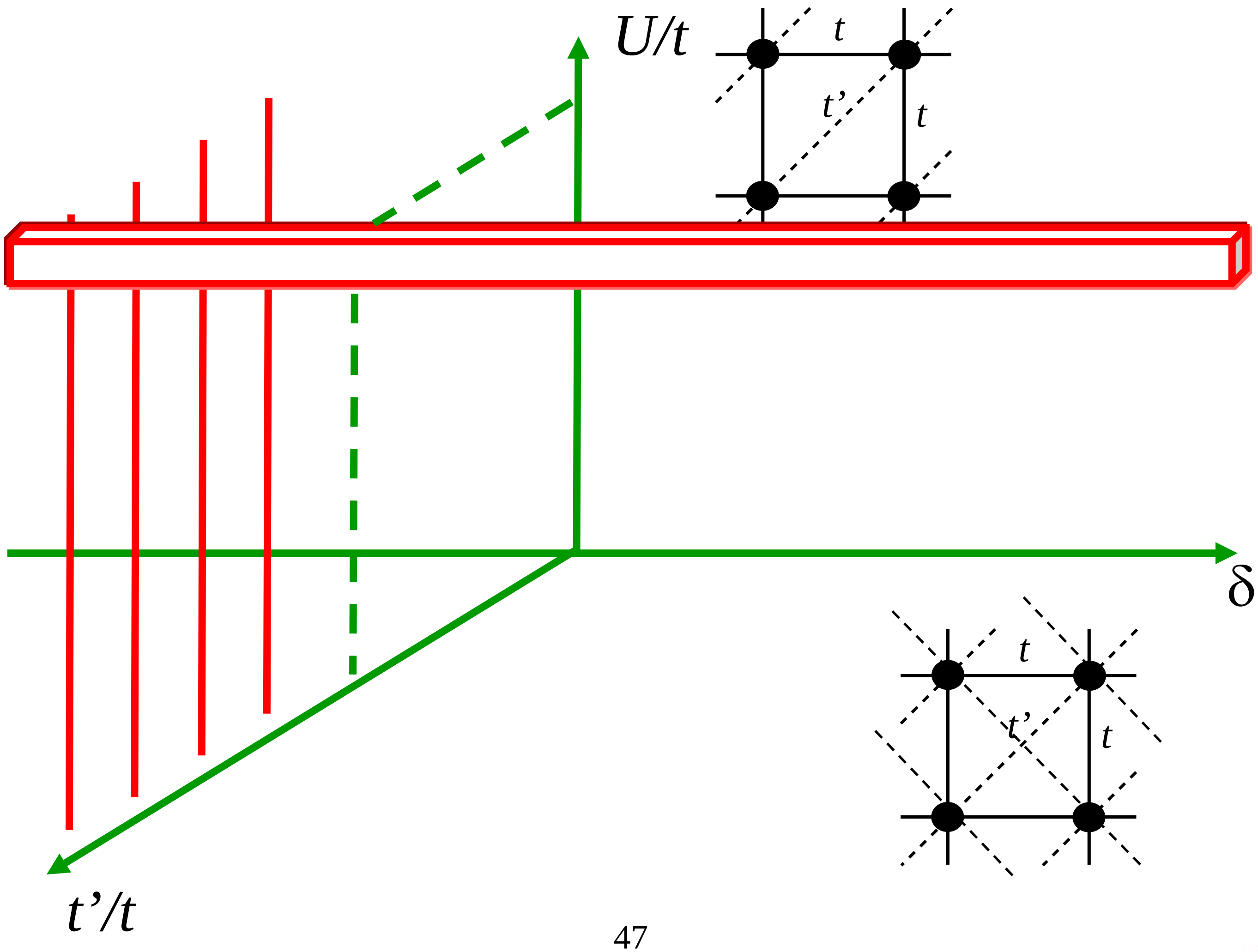

Solutions

- Bethe *ansatz* en *d=1* (correlation functions?).
- Groupe de renormalisation en une dimension (ou quasi-unidimensionnel) (Séparation spin-charge, Liquide de Luttinger)
  - *Solyom*, *Bourbonnais*
- Théorème de Nagaoka
- En deux ou trois dimensions (approx):
  - Approximation de Gutzwiller
  - Différentes formes de champ moyen pour bosons esclaves (+ champs de jauge).
  - ACDP
- Dimension infinie (Dynamical Mean-Field Theory)
- ……

C'est fini...

Merci